THE OFFICIAL MAGAZINE OF THE OCEANOGRAPHY SOCIETY

Oceanography

CITATION

Chavez, F.P., J.T. Pennington, R.P. Michisaki, M. Blum, G.M. Chavez, J. Friederich, B. Jones, R. Herlien, B. Kieft, B. Hobson, A.S. Ren, J. Ryan, J.C. Sevadjian, C. Wahl, K.R. Walz, K. Yamahara, G.E. Friederich, and M. Messié. 2017. Climate variability and change: Response of a coastal ocean ecosystem. *Oceanography* 30(4):128–145, https://doi.org/10.5670/oceanog.2017.429.

DOI

https://doi.org/10.5670/oceanog.2017.429

Climate Variability and Change

Response of a Coastal Ocean Ecosystem

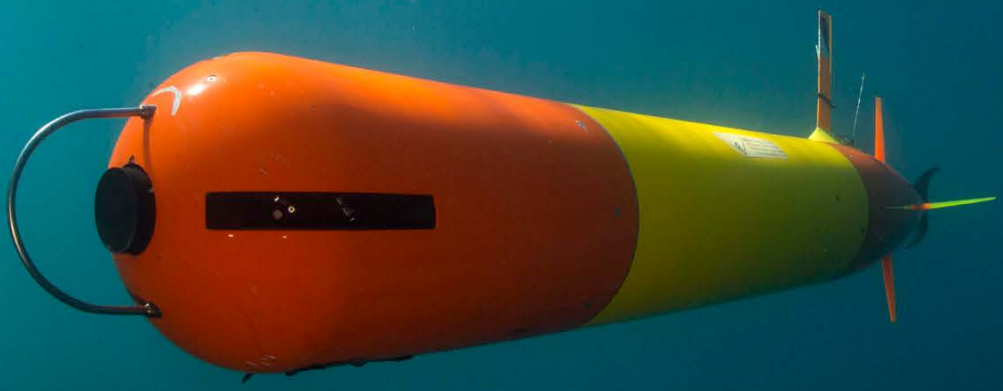

By Francisco P. Chavez, J. Timothy Pennington, Reiko P. Michisaki, Marguerite Blum, Gabriela M. Chavez, Jules Friederich, Brent Jones, Robert Herlien, Brian Kieft, Brett Hobson, Alice S. Ren, John Ryan, Jeffrey C. Sevadjian, Christopher Wahl, Kristine R. Walz, Kevan Yamahara, Gernot E. Friederich, and Monique Messié

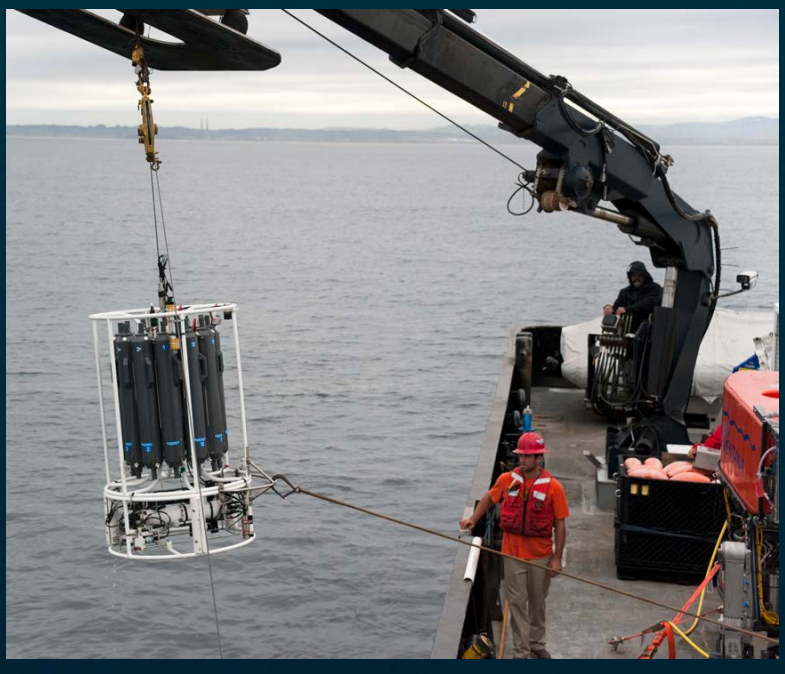

Background: MBARI Long Range Autonomous Underwater Vehicle designed to collect time-series measurements (credit: Kip Evans). Left photo: The M1 mooring just after deployment (credit: Francisco Chavez). Right photo: Time series CTD deployment on R/V *Rachel Carson* (credit: Todd Walsh).

> Time-series programs should themselves be subject to change, whenever it is necessary to do so.
>
> — Dave Karl, 2010

ABSTRACT. Monterey Bay and contiguous waters of the California Current System have been observed repeatedly since 1929, most intensively since 1989 with ships, moorings, and autonomous vehicles. Here, seasonal, interannual, and multidecadal variations are linked to regional weather and large-scale climate ocean-atmosphere dynamics. In the springtime, the Northeast Pacific subtropical high-pressure system strengthens, intensifying northwesterly alongshore winds. These winds drive coastal upwelling that fertilizes nearshore surface water with phytoplankton nutrients, resulting in a dramatic increase in biological productivity. Upwelling weakens over summer into fall, allowing nutrient-depleted offshore water to move toward the coast. Southerly winter storm winds deepen the mixed layer and further enhance onshore flow. El Niño interrupts these seasonal cycles with varying intensity every three to eight years, but typically peaks during the low-productivity winter season, lessening its biological impact. Over the 1989–2016 period of observation, a negative phase of the multidecadal Pacific Decadal Oscillation is observed as a 15-year cool period following the strong 1997–1998 El Niño. Two recently identified basin-scale phenomena, the central Pacific El Niño Modoki and the North Pacific Gyre Oscillation, increased in strength during this period. In Monterey Bay, primary productivity increased substantially during the cool period, at about 3% per year. This shift also marked the beginning of a monotonic decline in subsurface oxygen, which decreased by 3% annually in the 300–400 m depth horizon, above the oxygen minimum zone. Anthropogenically driven increases in surface pCO_2 and acidity (pH) are notable in Monterey Bay in spite of high near-surface variability. Recently, over 2014–2016, Monterey Bay has warmed, interrupting the 1988–2012 cooling trend. Even with the warm years included, however, there is no overall increasing trend in temperature at any depth from 1988 to the present. A recompilation of historical temperature data back to 1929 indicates that over this longer period, average and cool years have not been significantly different, but warm episodes have been hotter over the last few decades, leading to a trend of increasing temperature over the past 89 years. The 2014–2016 warm period included "the Blob" and an El Niño, and is reminiscent of similar conditions in the early 1940s. It is not known if the warm conditions will continue, or we will return to a cooler and drier than average period. Our observations highlight the value of long-term data. Such data collections will need to be automated to increase their value and sustainability.

INTRODUCTION

The lead author first visited Monterey Bay in 1985 when John Martin, then Director of Moss Landing Marine Laboratories, convened a meeting on the impacts of the 1982–1983 El Niño on the central California coast. We had just completed an intensive and purely serendipitous time-series study of the biological consequences of the 1982–1983 El Niño in the southeastern tropical Pacific off Peru (Barber and Chavez, 1983). The previous large El Niño of 1957–1958 had been interpreted by California scientists not as an interannual climate fluctuation but rather as the beginning of a long-term shift (Sette and Isaacs, 1960). It was not until several years later that Bjerknes (1966) linked global-scale atmospheric perturbations to the naturally occurring warm El Niño years off the coasts of Peru and California. The 1982–1983 El Niño, the strongest event of the century, spurred scientists globally to ponder if the intensity of this event had links to human-driven increases in atmospheric CO_2. Little did we know we would be back in Monterey Bay three years later, working to build a new oceanographic institution. The Monterey Bay Aquarium Research Institute (MBARI) was founded in 1987 following the 1984 opening of the Monterey Bay Aquarium. Since its inception, MBARI has supported long-term projects of oceanic investigation and technological development unsustainable under typical federal grant cycles. This special issue of *Oceanography* commemorates MBARI's first 30 years and celebrates the opportunity and effort that transformed David Packard's idea into an institute. Here we report on our team's work on variability in climate, circulation, and biological processes, and their combined effects on the transfer of energy through the food web and into the deep sea.

California and Peru share parallels as eastern boundary coastal upwelling systems (Chavez and Messié, 2009). Upwelling brings phytoplankton

nutrients to the well-lit surface layer, dramatically increasing primary productivity. Short food chains efficiently transfer solar energy to small pelagic fish so that coastal upwelling ecosystems produce more fish per unit area than any other regions in the world ocean (Ryther, 1969; Chavez et al., 2008). Sinking and decay of enhanced surface-derived primary production coupled with sluggish circulation lowers oxygen and increases carbon dioxide in subsurface waters relative to other ocean ecosystems. The upwelling of these low oxygen and pH, high pCO_2 waters makes surface waters in these regions on average lower in oxygen and more acidic than the open ocean. Finally, through ocean-atmosphere coupling, California and Peru are intimately linked to equatorial Pacific dynamics and subject to significant and coherent interannual (El Niño) to multidecadal (Pacific Decadal Oscillation) fluctuations in climate, ecosystems, and fisheries. Collapses of Monterey Bay and California sardine fisheries in the 1940s, and several decades later of the large-tonnage anchoveta fisheries off Peru, have been linked to such climate variability (Chavez et al., 2003).

Many decades after the collapse of its sardine fishery, Monterey Bay became a hotbed for ocean biogeochemical study. In the 1980s, John Martin and colleagues organized the VERTEX (VERtical Transport and EXchange) program that focused on biologically mediated transport of chemical elements from the surface to the deep sea. The VERTEX synthesis (Martin et al., 1987) provided impetus for the Joint Global Ocean Flux Study (JGOFS; Brewer et al., 1986). JGOFS supported process studies in globally important regions of the world ocean (e.g., equatorial upwelling, Southern Ocean) and established two time-series sites, one off Hawaii (Hawaii Ocean Time-series, HOT) and the other off Bermuda (Bermuda Atlantic Time-series Study, BATS). Building on our experience with time series off Peru during the 1982–1983 El Niño (Chavez, 1987), and as a contrast to the open-ocean sites, a similar time-series study was initiated in coastal Monterey Bay.

Monterey Bay provided an ideal setting, given its rich fisheries and oceanographic history. Time-series observations at station H3 in Monterey Bay were initiated by Hopkins Marine Station of Stanford University in the late 1920s (Skosberg, 1936). Hopkins scientists, the California Cooperative Oceanic Fisheries Investigations (CalCOFI), the Naval Postgraduate School (NPS), and Moss Landing Marine Laboratories irregularly sampled station H3 prior to the start of the MBARI Monterey Bay Time Series (MBTS) in 1988. We chose H3 as one of our core sites and established the M1 mooring near there in 1989. Semimonthly occupations of 11 stations in Monterey Bay were initially conducted. Over the years, the shipboard time series was refined to a three-station transect occupied at three- to four-week intervals. As autonomous systems were developed over the years, they have been incorporated into the time series.

The objectives of the time series were to (1) determine the mean and fluctuating components of phytoplankton primary production, biomass, and species composition on timescales ranging from days to decades; (2) determine the physical, chemical, and biological processes responsible for the mean and fluctuating components; and (3) determine the time-varying biogeochemical and ecological fate of primary production. The technology objectives were to (1) develop and deploy autonomous platforms and sensors to (2) increase both temporal and spatial resolution and (3) increase sustainability by reducing reliance on ships. In this contribution, we review scientific results, technology developments, and evolution of the time series over the period 1988–2016—almost 30 years.

ENVIRONMENTAL SETTING

The California Current System (CCS) occupies the region between the east-flowing North Pacific Current (~50°N) and the subtropical waters off Baja California, Mexico (~25°N) (Hickey 1979). The California Current is a broad, relatively shallow, wind-driven, equatorward-flowing surface current that represents the eastern limb of the North Pacific Subtropical Gyre. Inshore there is a swift surface equatorward coastal jet, and at depth the California Undercurrent flows poleward. In spring and summer, northwesterly winds drive coastal upwelling that brings cool nutrient-rich water to the surface, increasing biological productivity. Monterey Bay (~37°N) is near the center of the broadest (over 100 km) and most productive area of the CCS, spanning Cape Mendocino (~40°N) to Point Conception (~35°N). The CCS is highly variable on interannual and decadal timescales (Figure 1A–C), and Monterey Bay is subject to the same processes that drive the large-scale mean and variability for the entire CCS region. As a result, our time series tracks variations and trends in the CCS, the North Pacific, and the global ocean (see sections on El Niño, multidecadal variability, and trends).

An upwelling center off Año Nuevo Point (Figure 1D) is the primary source of cold, nutrient-rich water for Monterey Bay (Rosenfeld et al., 1994), although upwelling and/or mixing occurs along the entire region from Año Nuevo to Point Sur. Where upwelled water enters wind-protected portions of Monterey Bay, slower circulation and a warm and stable mixed layer foster dense phytoplankton blooms in a classical upwelling shadow environment (Ryan et al., 2008a; Chavez and Messié, 2009). The Monterey Bay upwelling shadow, separated from the cooler recently upwelled waters by a strong front, attracts a wide variety of sea life and is notable for the prevalence of harmful algal bloom species (Graham and Largier, 1997; Ryan et al., 2005, 2011, 2014, 2017; Jessup et al., 2009). Fisheries oceanographers refer to these shadows as biological action centers (Lluch-Belda et al., 2003). Monterey Bay served as an incubator for the sardine boom of the 1930s (Scofield, 1926, 1929) because biological productivity in such shadows is

high year-round, so that they serve as spawning and nursery grounds. The bulk of the water upwelled near Año Nuevo does not enter Monterey Bay but is vigorously advected offshore where nutrients are depleted more slowly and less completely than in the upwelling shadows (Chavez et al., 1991; Pennington et al., 2010).

The choice of the present-day time-series stations was guided by logistics and the physical and biological dynamics of Monterey Bay. The inshore site (C1) is a few kilometers from MBARI's dock in Moss Landing and is characteristic of the upwelling shadow environment, supporting high concentrations of phytoplankton (Figures 1E and 2D). Station M1 is located at the mouth of the bay in an area sampled since the late 1920s by scientists from Hopkins Marine Station (Skosberg, 1936; station H3), the California Department of Fish and Game (Scofield, 1929), and, later, CalCOFI (station 67-50). M1 typically lies within the Año Nuevo upwelling plume. Further offshore, station M2 is in less-productive waters that are more representative of the Coastal Transition Zone (CTZ). Shipboard sampling of C1 and M1 began in late 1988, and moorings were deployed at M1 and M2 in 1989 (see Box 1). Mooring M2 was removed in 2014, but the shipboard time series continues.

SEASONAL CYCLES

Monterey Bay oceanography follows the seasonal changes in atmospheric sea level pressure and associated surface winds over the Northeast Pacific. During spring, the North Pacific High expands and intensifies, and a broad thermally driven low-pressure area develops over the continent. The onshore pressure gradient in spring and summer intensifies equatorward winds along the central California coast (Pennington and Chavez, 2000) that drive equatorward transport and upwelling of deeper waters, two critical processes in Monterey Bay and the CCS. Equatorward winds drive surface ocean currents offshore, and the transported nearshore surface waters are replaced by cool, nutrient-rich waters from shallow depths (40–80 m) in a phenomenon known as coastal upwelling. Upwelling fertilizes the well-lit upper ocean and stimulates primary productivity. The spring transition from winter to the upwelling is often abrupt (see Strub and James, 2000), occurs in late February or March, and marks the beginning of cooler, high-nutrient and high-productivity conditions (Figure 2). Upwelling weakens in late summer into fall, and oceanic waters relax shoreward, compressing the productive upwelling region, concentrating prey, and attracting a wide variety of predators (Croll et al., 2005). Beginning about mid-October, winter storms intermittently break down the North Pacific High off central California, interrupting the upwelling process. The winter mixed layer is relatively deep (order of 50 m), with intermediate temperatures, fresher water, and low and uniform nutrients

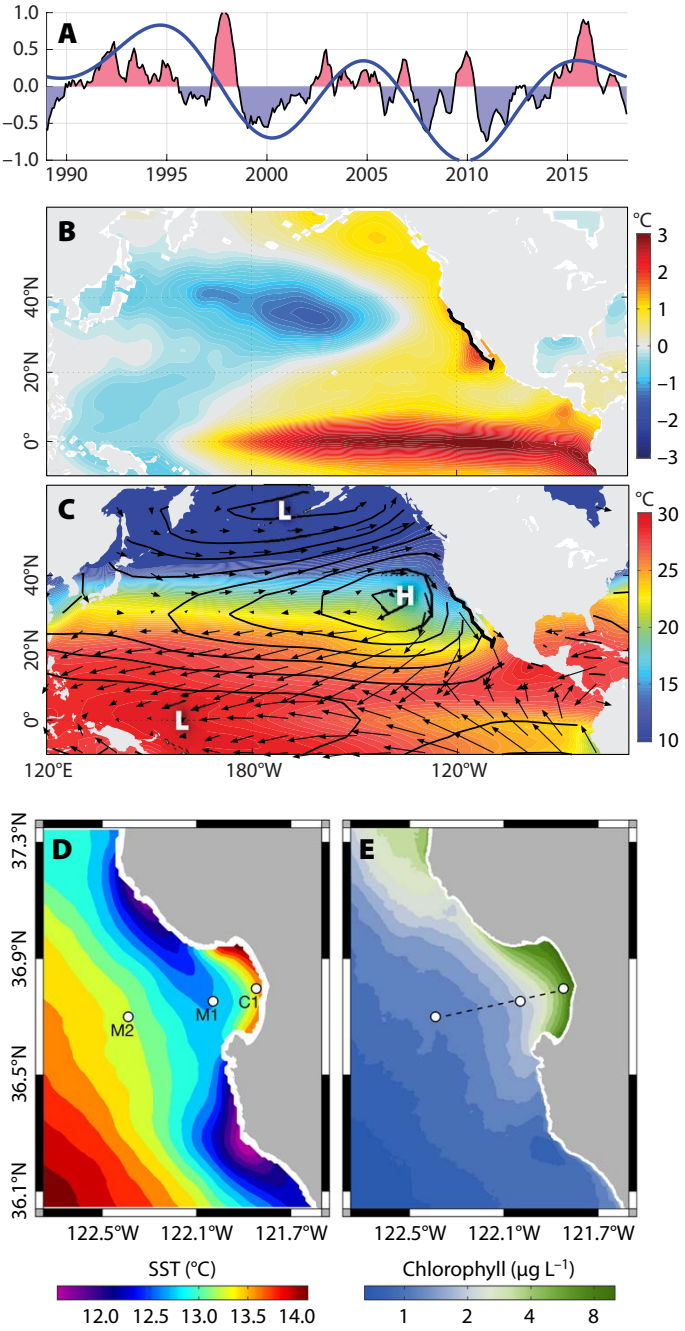

FIGURE 1. (A) First principal component of a global empirical orthogonal function (EOF) of sea surface temperature (SST) time series and its (B) spatial pattern plotted for the North Pacific (Messié and Chavez, 2011). The time series is highly correlated with the Multivariate ENSO (El Niño-Southern Oscillation) Index (MEI, r = 0.95), indicating that it captures El Niño. The smoothed blue line is the first principal component of a low frequency (periods of fewer than eight years suppressed) global time series, which correlates with the Pacific Decadal Oscillation (PDO, r = 0.65; Messié and Chavez, 2011). (C) Average SST, sea level pressure, and winds for the North Pacific. Notable are the Aleutian and Indonesian Lows [L], the North Pacific High [H], the cool California Current, and the North and South Pacific trade winds (see Chavez et al., 2011, for sources of data). (D) Average springtime SST. (E) Surface chlorophyll for Monterey Bay and the central California Current System with locations of time-series stations C1, M1, and M2, as well as the underway ship transect (dashed line).

and biological productivity. Skosberg (1936) named the oceanographic seasons described above as Upwelling (March–July), Oceanic (August–November), and Davidson/Winter (December–February).

Here, we use observations from 1988 to 2016 and compare seasonal cycles of physical, chemical, and biological parameters across the time-series sites. In Figure 2, we have suppressed high-frequency variability by heavily filtering the time series (four-month box car) and then creating annual averages. The physical properties were not remarkably different at the three sites, and we show M1 temperature and salinity series that nicely characterize the oceanographic seasons described above (Figures 2A and 3A). Coolest temperatures are found in April and warmest in September. Surface salinity increases from January to July, reflecting a slow and broad surfacing of the pycnocline resulting from continuing northwesterly winds and the increased transport of the California Current that flows well offshore (beginning order of 100–150 km; Collins et al., 2003). This geostrophic upwelling acts in concert with the local upwelling-favorable winds to fertilize the coastal ocean off Monterey Bay.

While temperature and salinity are similar among sites, the chemical and biological properties vary strongly (Figure 2B–H). M1, closest to and downstream of the upwelling center off Año Nuevo, displays the highest surface nitrate concentrations during the spring and summer upwelling season, while lower concentrations are found in the upwelling shadow at C1 and offshore at M2 (Figure 2B). In our coastal ocean, seasonal variations in nutrient chemistry and solar irradiance are key drivers of biological productivity. Nutrient uptake by phytoplankton reduces surface nutrient and carbon concentration, and the nitrate and pCO_2 seasonal cycles reflect a balance between supply by upwelling and removal via photosynthesis (Figure 2B,C). The highest concentrations of chlorophyll (phytoplankton biomass) are found inshore at C1, with intermediate values at M1 and lower values at M2 (Figure 2D). Levels of primary productivity (PP) are

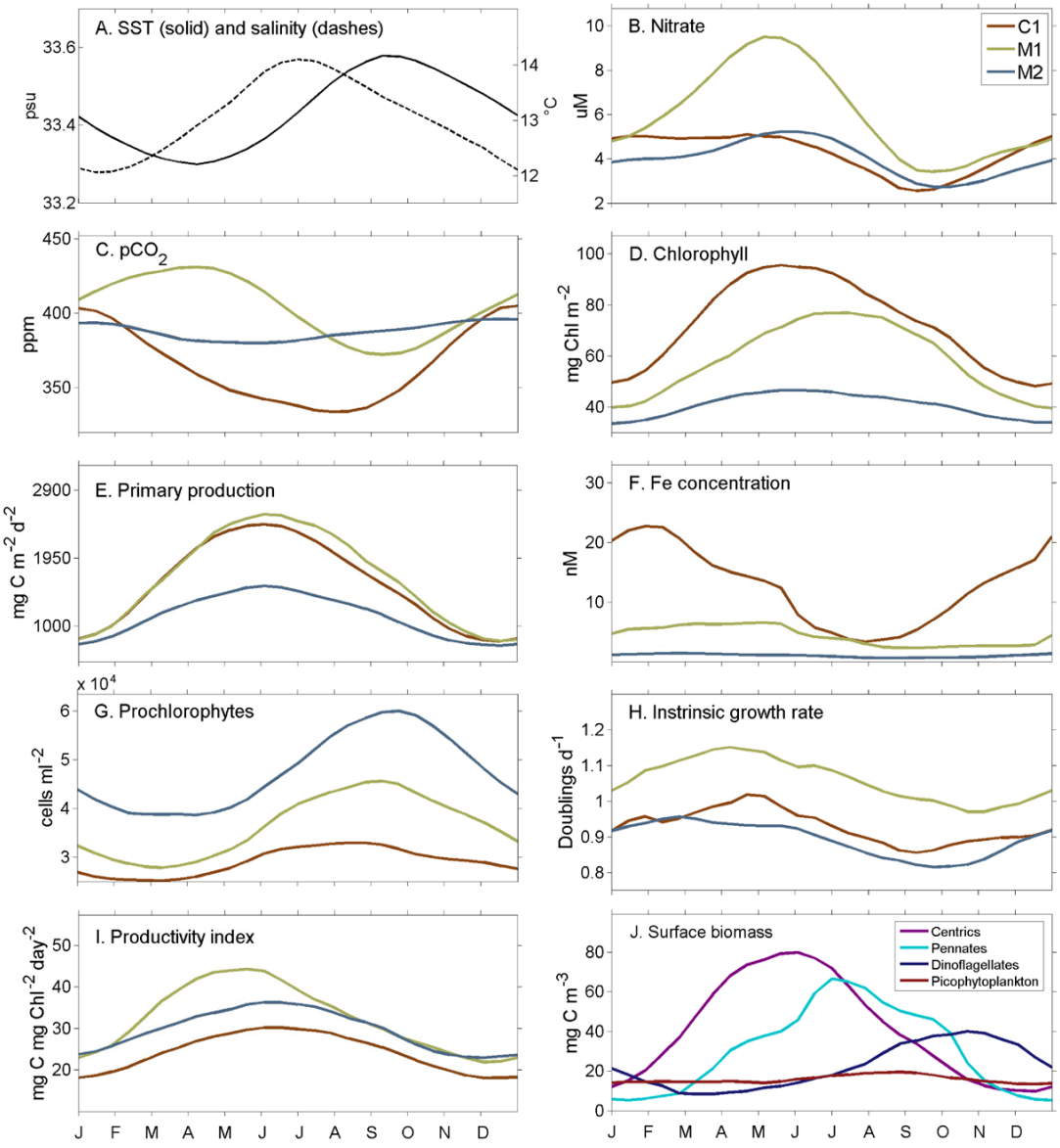

FIGURE 2. Climatological seasonal cycles of selected parameters from shipboard station occupations. Stations C1, M1, and M2 are brown, green, and blue, respectively, in panels B–I but not in A or J: (A) Sea surface temperature (solid line) and salinity (dashes) at M1. (B) Surface nitrate. (C) Surface pCO_2. (D) Euphotic zone-integrated chlorophyll. (E) Euphotic zone-integrated primary production. (F) Surface iron. (G) Surface prochlorophytes. (H) Phytoplankton growth rates, calculated using surface primary production and surface photosynthetic biomass as estimated from microscope counts of diatoms, autotrophic dinoflagellates, and picophytoplankton. (I) A phytoplankton "productivity index," calculated as surface primary production normalized to surface chlorophyll. (J) Surface biomass of centric and pennate diatoms, dinoflagellates, and picophytoplankton, average for C1, M1, and M2, estimated from microscope counts.

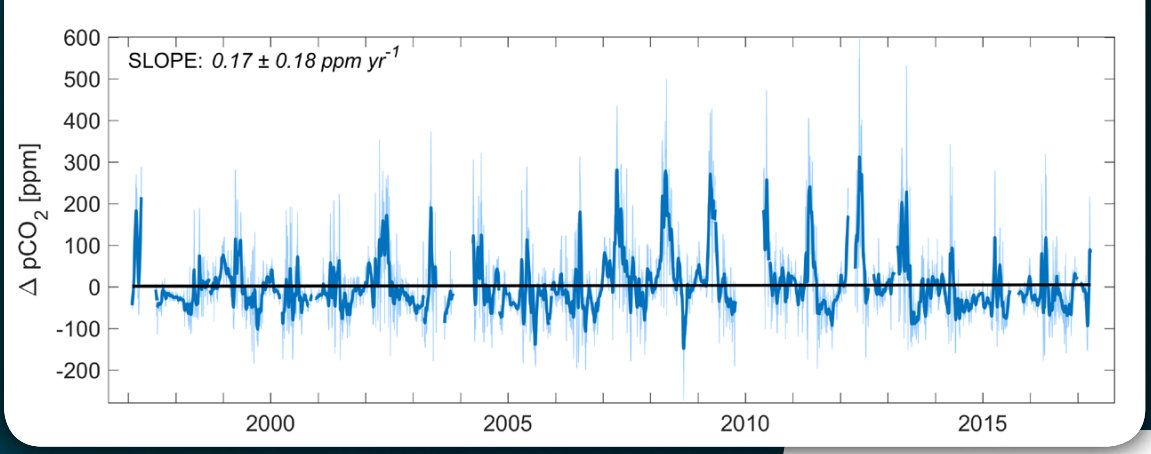

FIGURE B1-1. Time series of sea minus air pCO_2 (ΔpCO_2) measured at the M1 mooring using a system developed by Friederich et al. (1995) that has evolved over time. The slope of this time series is not significantly different than zero, indicating that the atmospheric increases in CO_2 are equilibrating with the surface ocean. The dark blue line has a 30-day low-pass filter applied. The seasonal upwelling with high sea surface pCO_2 in the spring and summer is evident. Also note the increasing highs in the record until the recent warm events.

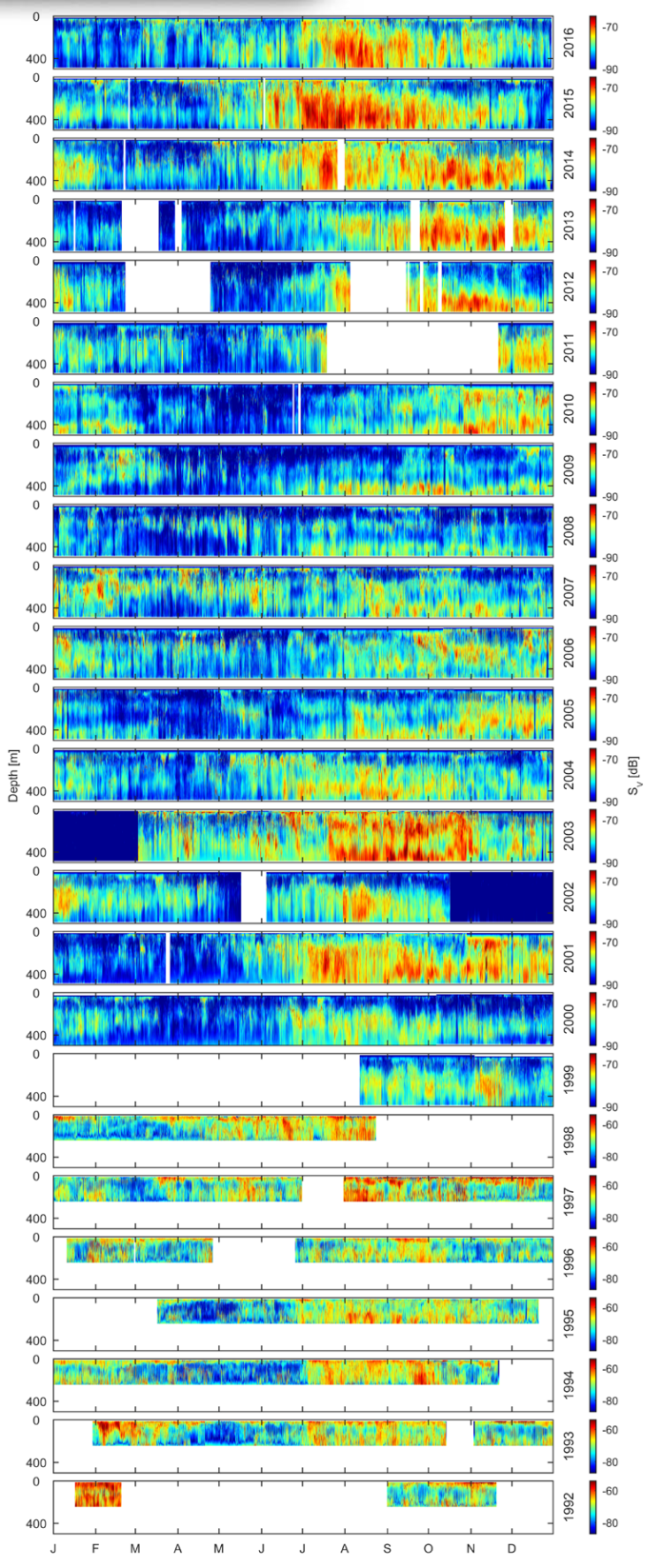

FIGURE B1-2. ADCP derived zooplankton backscatter at M1 from 1992 to 2016. From 1992 to 1996, the ADCP was a 150 kHz narrow band. From 1997 to the present, it has been a 75 kHz broadband.

Box 1. Moorings

MBARI's first autonomous platform was the M1 mooring, deployed in central Monterey Bay adjacent to the historical time-series station H3. M1 has been deployed nearly continuously since 1989. The mooring data are of high temporal resolution (10 minutes to 3 hours). Originally modeled on the ATLAS moorings of the Tropical Atmosphere Ocean (TAO) array (https://www.pmel.noaa.gov/gtmba), M1 has been extensively modified and carries suites of meteorological and oceanographic sensors (Chavez et al., 1997), including ocean and atmosphere pCO_2 (Figure B1-1), the in situ ultraviolet spectrophotometer (ISUS) nitrate sensor (Sakamoto et al., 2017, in this issue), and optical sensors (fluorescence, backscatter, downwelling irradiance, and upwelling radiance). M1 serves as a source of environmental data for the local and global communities and also as a platform for technology development and testing (Friederich et al., 1995; Johnson and Coletti, 2002; Johnson et al., 2006).

A downward-looking acoustic Doppler current profiler (ADCP) has been deployed on M1 since 1992, and its backscatter data provide a proxy record of zooplankton abundance (Figure B1-2). The record reveals (1) diel vertical migrations of scattering layers (not shown), (2) seasonal changes associated with development of the upwelling system in spring (cool colors, little backscatter) and contraction of the productive habitat in summer and fall (warm colors, more backscatter), and (3) interannual variability with low backscatter years (2004–2011) followed by high backscatter years (2013–2016). Counterintuitively, zooplankton appear to increase seasonally and interannually when upwelling decreases, allowing warm offshore waters to move inshore, compressing the productive habitat to M1 at the mouth of Monterey Bay.

very similar at M1 and C1, with seasonal maxima near the summer solstice (Figure 2E). Phytoplankton intrinsic growth rate as estimated from PP and phytoplankton biomass (Figure 2H) and the ratio of PP to chlorophyll (Figure 2I) show that on per cell and per unit chlorophyll bases, phytoplankton are growing faster at M1, consistent with M1 having optimal levels of nutrients (Figure 2B,F) and light. For C1 and M2, the rank order of productivity index (Figure 2I) and growth (Figure 2H) are reversed, with productivity index higher at M2 and growth rate higher at C1. This reversal is likely associated with cell size effects on the carbon to chlorophyll ratio. Inshore (C1), large phytoplankton with lower carbon to chlorophyll ratios dominate; smaller phytoplankton with higher carbon to chlorophyll are more important offshore (M2; Figure 2G). The dominant phytoplankton types in our time series are centric and pennate diatoms. Diatom abundance (Figure 2J), like PP, is highly correlated to the solar cycle with a maximum in June and July. As such, PP and diatoms are well correlated (r = 0.79); surprisingly, no other taxonomic group is well correlated with PP (picoplankton, dinoflagellates; Figure 2J). Centric diatom seasonality is clearly tied to springtime nutrients (Figure 2B) and light. However, as upwelling weakens and surface waters become more stratified, pennate diatoms increase and eventually dominate in late summer and fall. Pennates appear to be favored during intermediate upwelling conditions; thus, they can also be important in the spring during warmer, weaker upwelling years (Ryan et al., 2017). Pennate diatoms also are most abundant nearshore, suggesting a life-cycle relationship with the shelf (Chavez, 1989). Smaller organisms (picoplankton) also increase in abundance in the fall as warmer more oligotrophic waters are brought onshore during the seasonal upwelling relaxation (Figure 2). Dinoflagellate abundance is closely coupled to stratification as in other upwelling ecosystems (Margalef, 1978; Chavez, 1987) and is highest in late fall (Figure 2J). Relative to other phytoplankton types, picoplankton dominate during the winter as the larger phytoplankton decrease during deep mixed layer and low light conditions. Although Margalef (1978) did not include picophytoplankton in his famous "mandala," this seasonal distribution of phytoplankton types mirrors that he described for other coastal upwelling systems: (1) centric diatoms dominate with high nutrient and external energy input in spring; (2) as upwelling weakens and nutrients decrease, pennate diatoms become important; and finally (3) dinoflagellates are more important in stratified waters where turbulence is weak. In the Monterey Bay upwelling shadow, unusual conditions of high nutrient availability and strong stratification sometimes develop that favor red tide dinoflagellates that migrate down into the shallow nutricline at night and return to the surface to photosynthesize during the day (Ryan et al., 2009, 2010).

Respiration and warming also impact surface CO_2 levels. Inshore, particularly at M1, the seasonal cycle of CO_2 is surprisingly similar to that observed in the atmosphere, albeit with the ocean having a much larger amplitude. The light-driven seasonal cycle of photosynthesis in terrestrial environments draws CO_2 down in the atmosphere from spring to fall. By mid to late fall, terrestrial respiration exceeds photosynthesis. This continues through winter/early spring, increasing atmospheric CO_2 (Cleveland et al., 1983). In our coastal ocean, upwelling brings high-CO_2, high-nitrate, and low-oxygen waters to the surface during spring. These characteristics of upwelled waters result from the decomposition of sinking organic matter and associated respiration at depth. Following upwelling, phytoplankton bloom and net photosynthesis draws down CO_2 steadily from spring through summer, reaching a minimum in early fall. As upwelling weakens in the fall, and light reaching the ocean surface decreases due to shorter days and lower sun angles, respiration exceeds photosynthesis and CO_2 increases from fall through winter before reaching the upwelling maximum in spring. At our inshore site (C1), biological drawdown of CO_2 is greater in magnitude than at M1 (Figure 2B,C). CO_2 drawdown in the upwelling shadow exhibits a peculiar attribute, exceeding that predicted when complete uptake of nitrate is converted to carbon using a Redfield (1958) ratio. One explanation for this carbon overconsumption is "biological upwelling." Dense phytoplankton blooms develop in the upwelling shadow, often composed of vertical migrating dinoflagellates during late summer and fall (Ryan et al., 2008a,b; 2009, 2010). Our hypothesis is that these organisms undertake a nighttime "reverse migration" into the thermocline, where they take up nitrate and respire CO_2, and then return during daytime to sunlit surface waters, where they grow using the nitrate taken up at night, and reduce near-surface CO_2 to the observed levels. This biological upwelling creates a CO_2 deficit that is evident nearshore along the entire CCS in underway ship surveys of CO_2 (not shown). The seasonal cycle in CO_2 at M2 is much weaker than C1 or M1 (Figure 2C) and is characteristic of open-ocean waters of the CCS, which are more heavily influenced by the heat-driven solubility pump; warmer waters in fall have higher levels of CO_2.

The mean seasonal cycles have been well simulated with relatively simple models forced by wind-driven upwelling and light (Olivieri and Chavez, 2000). These canonical seasonal cycles vary from year to year because of the inherent interannual to multidecadal variability of the California Current System. In the following sections we remove the seasonal cycles and describe climate variability for the region (El Niño, Pacific Decadal Oscillation) together with anthropogenic trends. We transition from relatively well-understood seasonality and El Niño into emerging longer-term phenomena and more speculative impacts where we expect surprises that may well be counter to our present-day understanding.

EL NIÑO AND OTHER MODES OF CLIMATE VARIABILITY

Three basin-scale modes of interannual-to-multidecadal climate variability have had important impacts on Monterey Bay and the CCS over the past century: El Niño, the Pacific Decadal Oscillation (PDO), and the North Pacific Gyre Oscillation (NPGO). El Niño is the dominant mode of super-seasonal variability in Monterey Bay. El Niños originate in the equatorial Pacific, occur once every three to eight years with varying intensity, last between 12 and 18 months, and influence Monterey Bay and the CCS most intensely from October through March (Chavez et al., 2002b; Jacox et al. 2016; Figure 3). El Niño develops as follows. Easterly trade winds first reverse in the western Pacific during early fall (September to November) and then slacken across much of the tropical Pacific as the Indonesian Low migrates eastward. These westerly wind anomalies send upper-ocean Kelvin waves from the western Pacific along the equatorial belt to the South American coast that then travel poleward along the coasts of North and South America as coastally trapped waves (Enfield and Allen, 1980; Chelton and Davis, 1982; Parres-Sierra and O'Brien, 1989). These waves propagate to the Gulf of Alaska, deepening the thermocline; eventually, the surface waters along the North American coast warm further and stratify. Changes in the Indonesian Low, the largest and most persistent low-pressure system on the globe, also "teleconnect" to higher latitudes, and in the North Pacific result in a more intense winter and spring Aleutian Low and a weakened North Pacific High, amplifying the winter storm period and weakening the normal upwelling in the spring (Jacox et al., 2016). In combination, these atmospheric and oceanic impacts of El Niño produce warmer conditions in Monterey Bay and the CCS that favor subtropical, more diverse, and less productive food webs.

The average temperature cycle from 0 m to 200 m depth at station M1 over a May 1 to April 30 "El Niño year" is plotted in Figure 3A, and the first modes of variability of annual 0–200 m temperature anomalies from 1989 to 2017 are plotted in Figure 3B. The strongest warm anomalies (darker red) occur from November to February and are subsurface. Weaker warm anomalies extend into early spring (March and April). The first principal component and the Multivariate ENSO Index (MEI) are highly correlated (r = 0.79; Figure 3C); 62% of the temperature variance is explained by ENSO (El Niño-Southern Oscillation). Significant but slightly lower correlations are found between the MEI and annual 0–200 m nitrate (r = 0.76) and salinity (r = 0.71). High correlations with temperature were also found with the PDO (r = 0.72), weaker with the NPGO (r = −0.40). The NPGO was well correlated with salinity (r = 0.68) as previously noted by DiLorenzo et al. (2008). Weak correlations were found between all indices and chlorophyll and primary production. These weak correlations with biology are not surprising, given that winter is a period of low biological productivity and that summer, the seasonal productivity maxima, is weakly affected during El Niño.

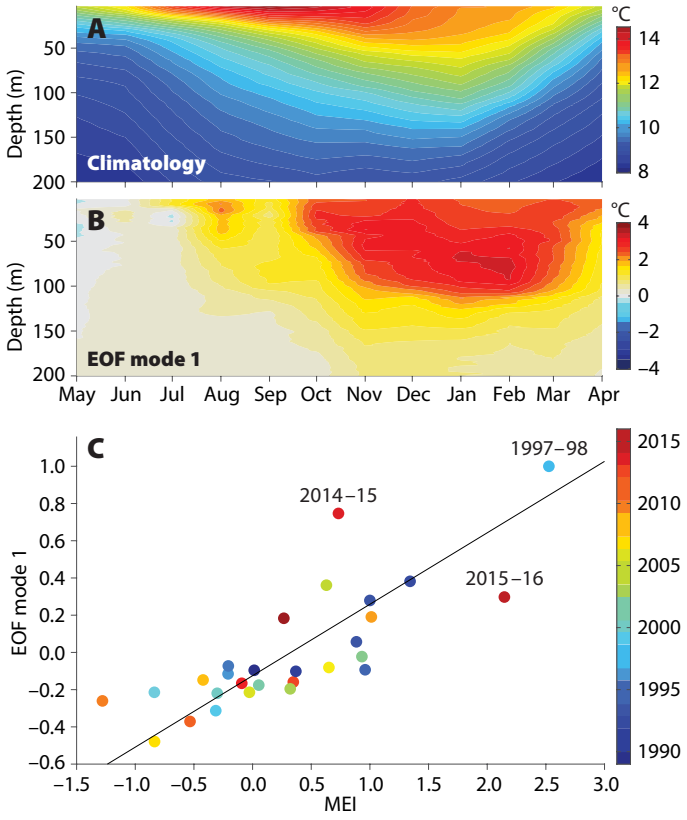

FIGURE 3. (A) Climatological 0–200 m temperature at station M1 plotted over an "El Niño year" beginning May 1. The data were obtained by two to three weekly shipboard occupations of M1 over 1989–2017. (B) The first EOF of annual 0–200 m temperature variability over the El Niño year. (C) The first principal component of temperature for each year (May 1 to April 30) plotted against the annual average MEI (r = 0.79). The correlation increases if the outlying warm Blob (2014–2015) and most recent El Niño (2015–2016) years are excluded.

A different statistical analysis of the M1 time series from 1988 to 2011 (Pennington and Chavez, 2017) reached similar conclusions for these indices and temperature, salinity, nitrate, chlorophyll, and primary production.

The weak correlations inshore between climate, chlorophyll, and primary production are related to nonlinear relations between physics and biology (Chavez, 1987). In recently upwelled waters, temperature, chlorophyll and primary production are low while nutrients are high (Barber and Smith, 1981; MacIsaac et al., 1985; Figure 4). Biological response to upwelling is fast—in three to four days, phytoplankton bloom and draw down nutrients. The cycle is complete when nutrients are fully exhausted, waters warm, and phytoplankton biomass and productivity decrease. The basic processes described above are illustrated in Figure 4 by showing integrated chlorophyll and productivity in relation to sea surface temperature and nitrate from over 1,700 measurements that extend into the California Current up to 300 km from shore. Primary productivity and chlorophyll are low in the coolest temperature bin (9°C), but they increase quickly, reaching a maximum over the next two temperature bins (10°C, 11°C), and then they decline monotonically. The

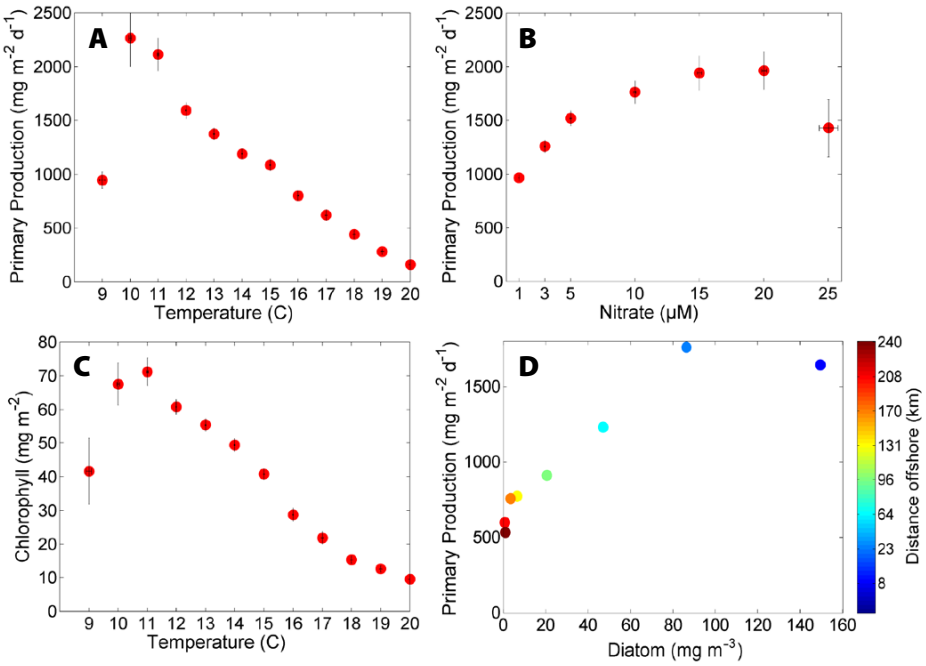

FIGURE 4. Primary production (PP), chlorophyll, diatom biomass, temperature, and nitrate relationships, using shipboard data from Monterey Bay to 300 km offshore in the California Current System. (A–C) Euphotic zone integrated PP and chlorophyll are low in newly upwelled, cold, high-nitrate water; highest in moderately cool water; and lowest in warm, low-nitrate offshore water. (D) Diatom biomass is high nearshore where PP is highest, and declines offshore, as does PP.

correlation between PP and temperature is high (r = 0.79) but increases significantly if we remove the low-temperature bin (r = 0.99). Chlorophyll has a similar increase in correlation with the low-temperature bin removed (from r = 0.84 to 0.98). A more dramatic increase is found in the relation between nitrate and primary productivity when the high-nitrate (low-temperature) bin is removed (r = 0.36 to 0.93). Average sea surface temperature at our time-series stations rarely reaches 15°C, leading to low correlations between temperature and chlorophyll and primary production. The expansion (cool) and contraction (warm) of the high-productivity zone also influences the relation between temperature and phytoplankton. The productive habitat broadens during La Niña and contracts during El Niño (Barber and Chavez, 1983; Chavez et al., 2002b). Weak upwelling and other coastal nutrient supply processes (canyon upwelling, land drainage) support the compressed habitat during El Niño and can further decouple nearshore temperature and productivity.

REGIME SHIFTS, THE 2013–2016 WARM YEARS, AND TRENDS

Time series of selected properties from 1998 to the present display the interannual variations discussed above (Figure 5). The large 1997–1998 El Niño, the 2013–2105 Blob, and the 2015–2016 period, all with very warm sea surface temperature (SST) anomalies and low nitrate, are notable. Also prominent are the decade-long period of generally warmer, lower chlorophyll and nitrate waters prior to 1997 that include the weaker but more prolonged 1992–1993 El Niño and a period of prolonged cool anomalies after. The prolonged cooling, and higher chlorophyll and nitrate that followed the 1997–1998 El Niño resulted in trends of decreasing temperature and increasing nitrate and primary production (Pennington and Chavez, 2017). This prolonged cooling was associated with a long-term increase in the large-scale Pacific trade wind field, a hiatus in global warming, and a shift in the PDO (Chavez et al. 2003, 2011; England et al., 2014). The multi-decadal cooling was evident over a triangle stretching from the Pacific Northwest to the dateline to the coast of Chile (Chavez et al., 2011). The large-scale nature of the cooling indicates that it was not related to mesoscale intensification of coastal upwelling associated with the global warming as predicted by Bakun (1990). The magnitude of the 1990s shift was such that it increased the amplitude of two previously unrecognized climatic phenomena: (1) El Niño changed in character, from an eastern Pacific warm anomaly to a central Pacific Modoki warming (Ashok et al., 2007), and (2) the NPGO intensified and was first described (DiLorenzo et al., 2008). The NPGO is characterized by a horseshoe-shaped pattern of anomalous sea surface temperature (warm or cool) extending from the central equatorial Pacific northeastward to the California coast and Alaska, and then back around to Japan.

The extended cool period was abruptly interrupted in late 2013, 2014, and 2015–2016 when Monterey Bay warmed dramatically, unlike anything seen since the early 1940s (Figure 5; Brönnimann, 2005). The 1940s warm period was followed by several decades of cooler than average conditions that have been associated with the collapse of California sardines (Chavez et al., 2003). In late 2013, surface oceanic water within the NPGO horseshoe became unusually warm, a phenomenon that became known as the Blob (Bond et al., 2015). The Blob spread and pushed into Monterey Bay beginning in mid-2014. The warmest SST ever observed at the M1 mooring was measured during October 2014. The 2014–2015 El Niño year was the second warmest in our record, only behind 1997–1998, yet the MEI was not unusually high (Figure 3C). The Blob waned in mid-2015 but was immediately followed by the 2015–2016 El Niño. This El Niño was unusual in that it was "strong" based on the MEI, second only to 1997–1998 (Figure 3C) but relatively weak in Monterey Bay (Figure 3C). The "Godzilla" El Niño rains predicted for California did not materialize but significant marine ecosystem disturbances did. This event has been characterized

as a hybrid between the classical eastern Pacific El Niño and the central Pacific El Niño Modoki (Paek et al., 2017). The heavy rainfall predicted for the 2015–2016 winter instead appeared during the 2016–2017 winter. A surprising increase in precipitation also occurred in northern Peru in early 2017, with catastrophic flooding and SST anomalies of 10°C, and again without a large-scale El Niño.

The phenomena described above are evident in the Monterey Bay time series of temperature, nitrate, chlorophyll, and oxygen (Figure 5). Prior to the recent warm years, the trends in Monterey Bay temperatures over the 1989–2011 period indicated the general decadal cooling that was evident over the eastern and equatorial Pacific (Chavez et al., 2011; England et al., 2014; Pennington and Chavez, 2017). When the last few years of data are included, however, the overall Monterey Bay 1988–2017 temperature trend is not significantly different from zero at all depths from 0 m to 200 m. The reported increases in salinity, nitrate, chlorophyll, and primary production (Pennington and Chavez, 2017) are still found, although reduced in particular for salinity and nitrate. Primary productivity continues to increase, now at a rate greater than 1% per year, but down from the very substantial 3% per year observed between 1989 and 2011.

The observed increasing trends in PP are associated with a parallel increasing trend in phytoplankton growth rate, as estimated from PP and phytoplankton biomass (from microscopy) or chlorophyll. This indicates that phytoplankton biomass and chlorophyll are stable, or are increasing at a slower rate than PP. Surprisingly, centric diatom biomass did not increase during the cool decades, but pennate diatom and dinoflagellate biomasses exhibited late summer and fall increases (MBARI, 2010). The slower rates of increase of phytoplankton biomass and chlorophyll may be related to upwelling intensity and the size of the productive habitat, as discussed above. During cooler strong upwelling periods, the size of the habitat is large as high-nutrient waters are advected far from shore. The broad nearshore area has optimal light and nutrient levels, and phytoplankton growth rate is enhanced. Iron or nutrient levels (see below in relation to declining oxygen) may also be responsible for the observed increases in PP. Iron data collected on the time-series cruises from 1998 to 2005 (Elrod et al., 2008) indicated a close coupling between iron supply and phytoplankton growth during early upwelling (Johnson et al., 2001). Increased iron supply during the cooler, stronger upwelling period could have driven the higher phytoplankton growth rates.

A particularly striking change after 1997–1998 has been a persistent decrease in oxygen at depth (26.8 isopycnal, 300–400 m; Figure 5D). The decrease is consistent with that reported by Bograd et al. (2008) for Southern California. Comparison of Monterey Bay changes with those from southern CalCOFI lines (not shown) indicate that oxygen at depth was stable from 1988 to 1997–1998, and then began a steady decline that appears to have slowed during the recent warm period. Ecosystem changes in deeper water biota with affinities for lower oxygen, such as the giant squid *Dosidicus gigas* (Figure 5E), were also evident after 1997–1998 (Zeidberg and Robison, 2007). A comparison of 2003 and 2012 hydrographic sections made along the 1,000 m isobaths from Monterey Bay to

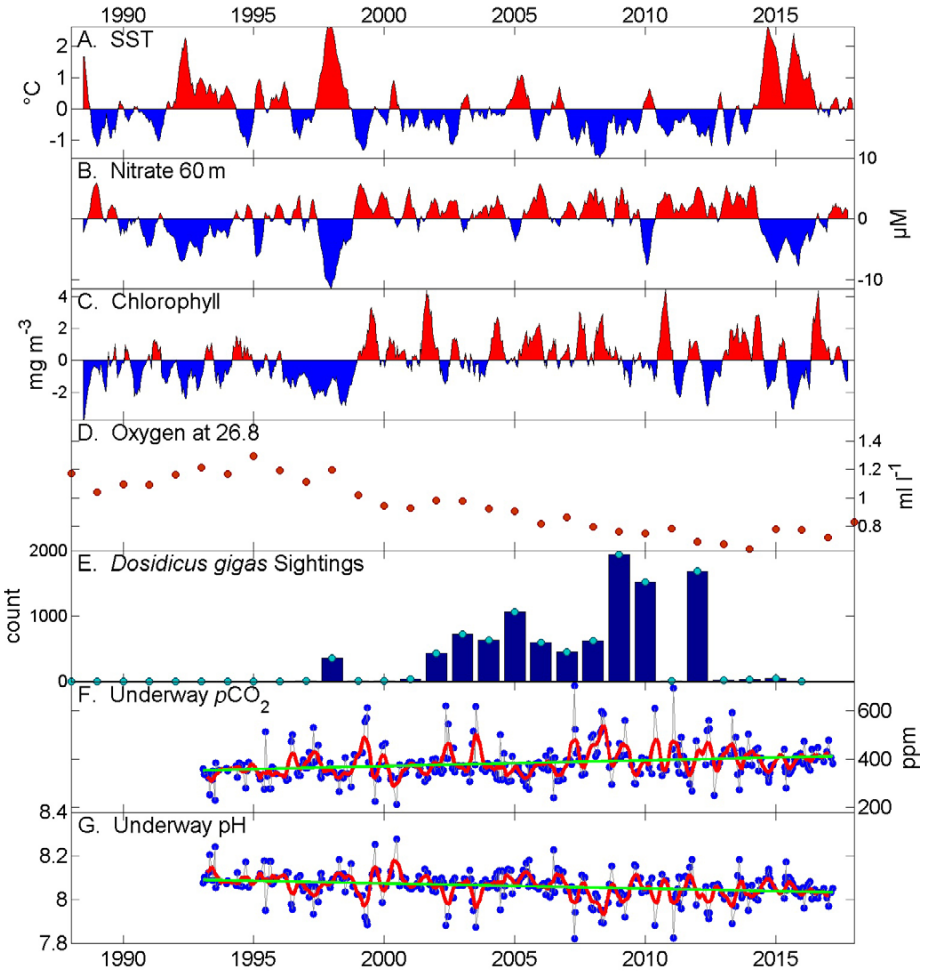

FIGURE 5. Time series of Monterey Bay properties, 1989–2017: (A–C) Nonseasonal anomalies of SST, 60 m nitrate, and surface chlorophyll averaged over stations C1, M1, and M2. Anomaly calculation in Pennington and Chavez (2017). (D) Average annual oxygen at σ_t = 26.8. (E) Submarine (remotely operated vehicle) sightings of jumbo squid *Dosidicus gigas* in the Monterey Bay region. (F–G) Shipboard measured pCO_2 and estimated pH every two to three weeks from the transect shown in Figure 1E. The pH was calculated from pCO_2 and salinity-derived alkalinity estimates.

Cabo San Lucas show decreased oxygen in 2012 along the entire transect, with maximum decreases between 50 m and 300 m (Figure 6). When we compare the differences between the two cruises in terms of oxygen, total CO_2, and nitrate, we find that the deeper oxygen decrease is associated with increases in CO_2 and nitrate at their respective Redfield ratios (Figure 6). The oxygen decrease is thus associated with increased respiration and organic matter remineralization in subsurface CCS waters, driven by either enhanced vertical export of surface primary production (enhanced biological pump) or weaker large-scale replenishment (or ventilation) of low-oxygen waters from high latitudes (Ren, 2016). Rykaczewski and Dunne (2010) predict increases in primary production in the CCS in a warmer world based on weaker ventilation and associated nutrient increase. Are the primary productivity increases we report above associated (1) with increased deepwater nutrients due to weaker ventilation, or (2) with the general shoaling of the thermocline/nutricline driven by the trade wind intensification? And are the two related? CCS variations in oxygen at depth have a clear multi-decadal signature (McClatchie et al., 2010; Deutsch et al., 2014), and it remains unclear if the recent observed decreases in subsurface oxygen are driven by multi-decadal variability (in biological productivity or ventilation) or by longer-term global-warming-driven changes in ventilation. The vertical distribution of declining oxygen off Monterey Bay estimated from the time series suggests that both productivity and ventilation processes may be at work (Figure 7A). The absolute rate of decrease shows peaks at about 80 m and 300 m. The shallow peak, just beneath the pycnocline, is indicative of local increases in remineralization. The deeper peak, decoupled from the shallow one, has to be associated with changes in large-scale circulation and ventilation. While of similar absolute values, the deeper peak is

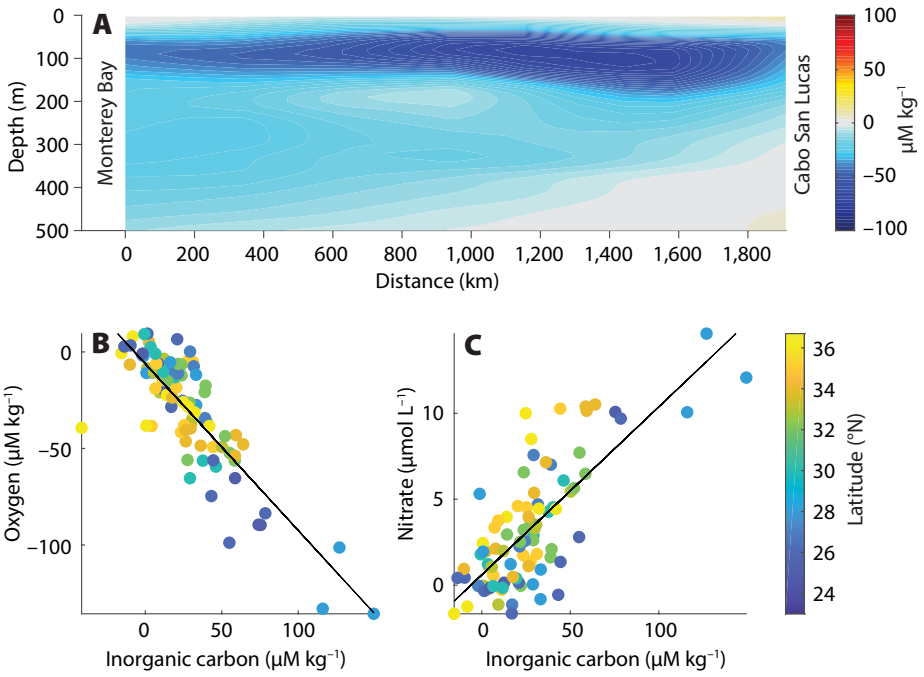

FIGURE 6. Deepwater oxygen decreased and dissolved inorganic carbon (DIC) and nitrate increased from 2003 to 2012 between Monterey Bay and Cabo San Lucas. Data are from cruises in February 2003 and 2012. (A) The plot shows the difference in oxygen between 2003 and 2012. In 2012, oxygen was much reduced over 50–350 m depth, consistent with Figures 5 and 7 and reports by Bograd et al. (2008). (B–C) Plots show the differences in oxygen, DIC, and nitrate at 50–500 m depth between 2003 and 2012. DIC and nitrate both increased with reduced oxygen, regardless of latitude. Regression slopes are near their respective Redfield ratios.

FIGURE 7. Vertical profiles of the (A) absolute and (B) percent rate of oxygen change for the region from the M1 mooring to 300 km from shore over 1998 to 2013. Above ~500 m depth, oxygen levels have decreased notably, with a shallow peak near the base of the thermocline that is associated with a shallower thermocline/oxycline and an enhanced biological pump during the cool and productive years following the 1997–1998 El Niño. The deeper decline, centered on the 26.8 isopycnal, is likely associated with the shallow meridional overturning circulation that ventilates the region with high-latitude waters of the North Pacific. On a percentage basis, the deeper peak has the largest rate of change at over 3% per year. Beneath ~500 m in the oxygen minimum and below, levels have increased over the same time period. Similar estimates from the Monterey Bay to Gulf of California transects (Figure 6; dashed lines) are also plotted. The shape of the profiles are nearly identical except that the Gulf of California transect shallow peak is more intense. These independent observations indicate that Monterey Bay observations are representative of large-scale conditions in the CCS.

much larger in relative values, in excess of 3% oxygen reduction per year. The data also indicate an oxygen increase within the oxygen minimum zone (OMZ; 600–800 m) and below (Figure 7B). Paleo sedimentary oxygen records indicate an expansion of OMZs during warm interglacial periods but an oxygenation of the very deep ocean (Jaccard et al., 2014). The same calculations performed on the Gulf of California transect (average of oxygen profiles from Monterey Bay to Cabo San Lucas) show nearly identical results except that the surface peak is enhanced in the Gulf of California transect (Figure 7, dashed lines). The independent calculations indicate that the Monterey Bay data are representative of large-scale changes in the CCS.

Shipboard underway measurements of sea surface pCO_2 have been collected since 1993 (Figure 8), and the M1 mooring was equipped with an autonomous sea surface pCO_2 system starting in 1997 (Box 1). These records represent the longest marine time series of their type. Strong intraseasonal to interannual variations are evident in the time series of pCO_2, but a statistically significant increase of surface CO_2 can nevertheless be detected. pCO_2 is increasing at 2.39 ppm per year, at a rate slightly faster, but not significantly different, than the 1.97 ppm per year CO_2 increase observed in the atmosphere at the Mauna Loa observatory over the same period (Figure 8). The trend in the mooring time series of delta pCO_2 is very slightly positive (0.2 ppm per year) but not significantly different than zero, also indicating that CO_2 in the surface ocean has been increasing at a rate similar to CO_2 in the atmosphere, providing unequivocal evidence of the ocean's absorption of atmospheric CO_2. When the pCO_2 time series is converted to pH and compared to that measured at the Hawaii Ocean Time-series site, the two time series show a significant decline in pH, with Monterey Bay at 0.0024 and HOT at 0.0014 pH units per year (Figure 8). On average, the surface pH of Monterey Bay is 0.1 pH units lower than HOT, reflecting the upwelling of higher pCO_2 (lower pH) water. The declining oxygen trend discussed above also contributes to increasing concentrations of CO_2 in upwelled waters. We can estimate this contribution based on the oxygen decline to result in a 4 µM per year increase in total CO_2 in upwelled source waters, leading to an increase in pCO_2 of 8 ppm and a decrease in pH of 0.08. These increases are larger than those estimated from rising atmospheric CO_2. Because nitrate at depth is also increasing and enhancing photosynthesis, the net effect on pCO_2 and pH should be close to zero when integrated over the full upwelling system. However, higher pCO_2 nearshore in the upwelling zone is predicted, and the mooring time series shows increasing concentrations in the highest pCO_2 values over time (excluding the recent warm years; Figure 8). These higher pCO_2, lower pH waters over the CCS have had direct negative impacts on the calcareous shellfish industry (Barton et al., 2012).

A surface temperature record at or near our M1 station was assembled from 1929 to the present (Figure 9). Scientists at Hopkins Marine Station collected data from 1929 to 1933 (Skosberg, 1936). A long hiatus followed, and measurements were started again when the CalCOFI program began in the early 1950s after the sardine fishery collapse. The CalCOFI program retreated to Southern California in 1978, and sporadic occupations occurred from then until 1988 when the MBARI time series was initiated. A regression using all of the data results in a positive increasing temperature trend (<0.1°C per decade). Annual means (red dots) suggest that this trend is driven by a few very warm years in the recent record. Recent cool or average years are not significantly different

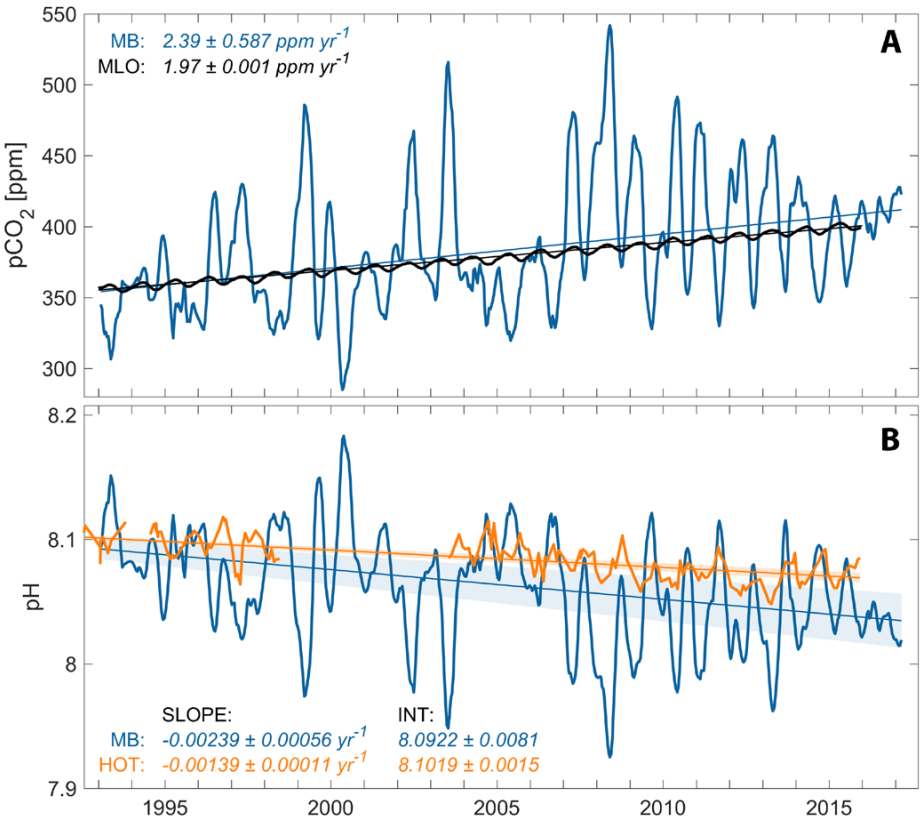

FIGURE 8. (A) Time series of underway surface pCO_2 and (B) surface pH estimated from (A) and alkalinity derived from salinity, plotted with atmospheric CO_2 at Mauna Loa and Hawaii Ocean Time-series (HOT) pH, respectively. The sea surface pCO_2, while not significantly different than that of the atmosphere, is increasing at a slightly faster rate likely related to the general cooling and declining oxygen in surface waters after 1997–1998, and consistent with pCO_2 measurements in the equatorial Pacific (Sutton et al., 2014). Monterey Bay pH is on average 0.01 units lower than HOT due to the upwelling process, and is also declining at a slightly faster rate.

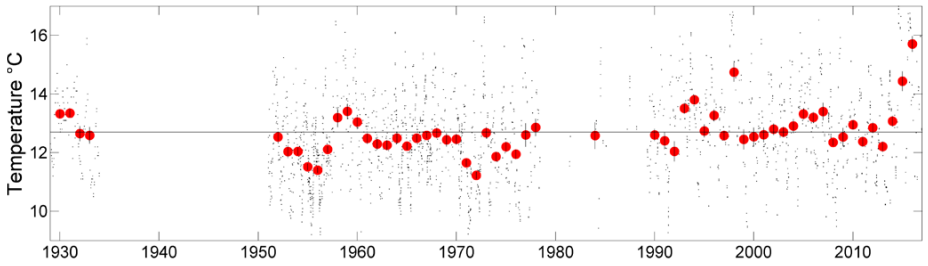

FIGURE 9. Sea surface temperature measurements made at or near the Station H3/M1 mooring from 1929 to 2017. The small black dots are single measurements; the large red dots are annual averages over the El Niño year of May 1 to April 30 (Figure 3). Monthly means were first calculated and then averaged annually. Years with sparse coverage (<8 months) were not included. The thin black line is the average of all years (12.7°C). There is a positive trend to the time series (<0.1°C per decade) when all of the data are included. The annual means suggest that this trend is driven primarily by a few very warm years in the recent record. Recent cool or average years are not significantly different from those measured at the beginning of the record.

from those measured at the beginning of the record (Figure 9). We note that the large warm anomaly in the early 1940s is missing from this record.

THE FUTURE IN THE AGE OF UNCERTAINTY

For almost 30 years, we have made shipboard measurements of physical, chemical, and biological parameters in Monterey Bay and the California Current System. These high-quality data sets have been augmented by a sensor and platform development drive to automate data collections, first by producing high-frequency time-series data from moorings (Chavez et al., 1997; since 1989), and more recently with high-spatial-resolution data sets collected by autonomous underwater vehicles (AUVs) in Monterey Bay since 2003 and gliders since 2007. These data sets now span many temporal and spatial scales against which change can be measured. In the early years, we described the seasonal and spatial pattern of the physics, nutrient chemistry, and primary production, providing a detailed understanding of euphotic zone dynamics in Monterey Bay (see references in Chavez and Collins, 1998, 2000). In the 1990s we encountered El Niño and La Niña, and documented their impacts in central California (see references in Chavez et al., 2002a) and the equatorial Pacific (Chavez et al., 1999), contributing to the realization that global climate fluctuations cause dramatic changes in our local ecosystems. And finally, following the 1997–1998 El Niño, our data indicated that Monterey Bay had cooled—only slightly, but still enough to significantly affect local ecosystem dynamics (Chavez et al., 2003; Pennington and Chavez, 2017). This multi-decadal regime shift was one of the most significant of the past century (Chavez et al., 2011). More recently, we encountered the warm Blob, followed by El Niño. Our analysis indicates that the central California environment follows the Pacific basin rather closely. Data from our Monterey Bay time series and from HOT, which are contrasting but linked sites, show that both ecosystems are regulated by the North Pacific climate and gyre circulation (Chavez et al., 2011; Karl and Church, 2011). Picoplankton dominate the oligotrophic HOT, while diatoms dominate the eutrophic Monterey Bay. These sites seem to oscillate out of phase with each other; productivity at HOT increases during El Niño and during the warm phase of the Pacific multi-decadal variability (known as El Viejo, the old man, a play on El Niño), while Monterey Bay does the opposite (Chavez et al., 2011).

Anthropogenic impacts and recent enhanced and unexplained variability indicate that the need for measuring ocean change is more important than ever. Recent warming events remind us once again that many aspects of ocean ecosystem dynamics have yet to be fully understood. Given rapid changes occurring in the Earth system relative to historical records, we are in an age of uncertainty in which past experiences may no longer be of use to predict the future. How fast and in which direction will climate change in a warmer world? Will the ocean continue losing oxygen and how fast? Will we have more harmful algal blooms? Will temperate ecosystems become more tropical? What will happen to the overall health of the ocean? Answers to these basic questions require continually updated information on ocean ecosystem conditions. With a renewed emphasis on sensor development and process studies, we now strive to move to a mostly autonomous time series (Figure 10). The M1 mooring provides an anchor for the time series, but it is clear that a larger spatial footprint is required.

Over a decade ago, MBARI entered into the world of autonomous vehicle research and development. The first forays were devoted to gaining experience with gliders and 12-inch class AUVs. The large-class AUVs have been modified for water column and benthic studies. An important development in the water column AUVs was the capability to collect water and return it to shore for laboratory analysis (Ryan et al., 2010). Recently, we demonstrated that water from AUVs could be analyzed for many of the same properties (temperature, salinity, oxygen, nutrients, chlorophyll, primary production, species composition) that are collected using ships (Pennington et al., 2016; see Boxes 2 and 3). These larger AUVs also have limitations in that they are expensive, they require ships for deployment and recovery, and their mission durations are short, on the order of a day. To fill a void between the long-duration, small-payload gliders and the short-duration, high-payload 12-inch AUVs, MBARI developed a new class of vehicle, the so-called Long Range AUV (LRAUV; Bellingham et al., 2010; Hobson et al., 2012). The capabilities and use of the LRAUVs has been refined under process-oriented coordinated

Box 2. Autonomous Vehicles

Autonomous vehicles can greatly increase measurement resolution. At MBARI, the capabilities of autonomous systems have been refined under process-oriented coordinated campaigns with fleets of vehicles (Figure B2-1). These systems can now operate 24/7 and are essentially impervious to weather; each platform is monitored remotely and produces data densities several orders of magnitude greater than can be achieved by shipboard profiling CTD. An example is provided for gliders that have been operating along CalCOFI Line 67 off Monterey Bay since 2007 (Rudnick et al., 2017; Figure B2-2). Excluding development costs, autonomous platform values and operating costs are about an order of magnitude lower than those of shipboard work.

A wide variety of analyses (biology and chemistry) are currently done with water collected using Niskin type bottles on the cruises, but water samplers have now been built for both large and small autonomous underwater vehicles (AUVs). Validation of AUV samples suggests they are remarkably good for a basic suite of properties (Pennington et al., 2016; Figure B2-3). The adaptation of a new generation Environmental Sample Processor (ESP) to the Long Range AUVs opens new opportunities for process and time-series studies (see Scholin et al., 2017, in this issue).

FIGURE B2-1. Fleet of six Long Range AUVs with a Wave Glider prior to deployment in support of an interdisciplinary experiment in Monterey Bay during May 2017.

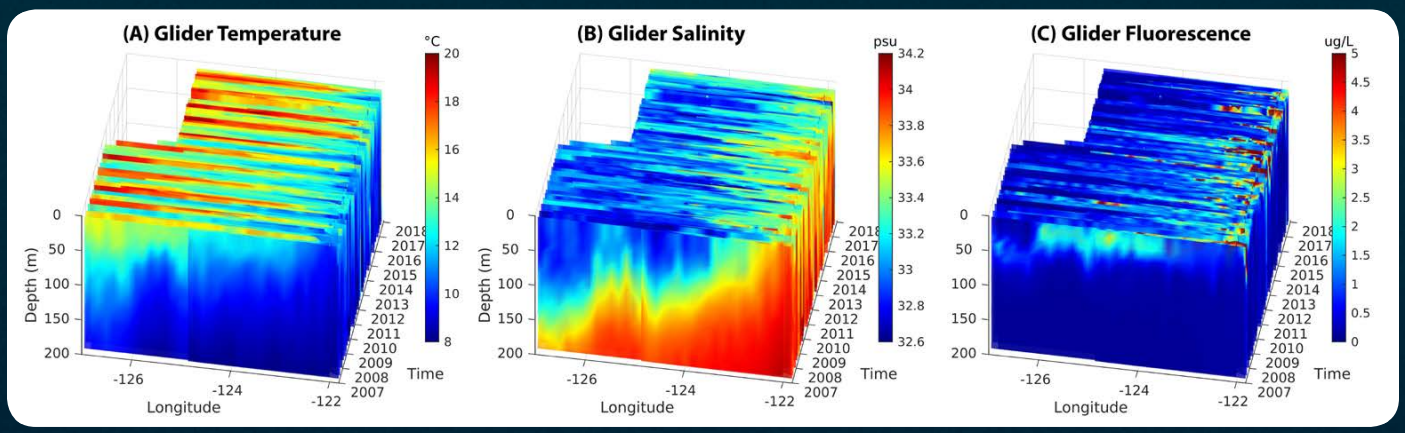

FIGURE B2-2. Since 2007, profiling gliders have extended the time series transect 300 km offshore. In the stacked temperature, salinity, and chlorophyll fluorescence sections, the doming of the thermocline from offshore to inshore is notable (volume of cooler blue increasing from left to right) as is the southward flow of the low salt California Current offshore (blues to upper left) and the high chlorophyll nearshore.

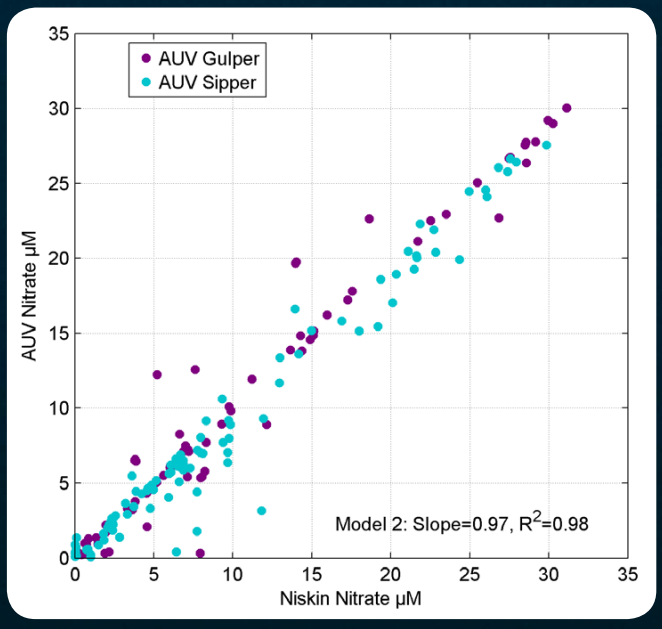

FIGURE B2-3. Nitrate analyses from AUV-collected Gulper (large AUV) and Sipper (small, long-range AUV) water samples compared to ship-collected Niskin bottles.

Box 3. Observing Life in the Sea (Figure B3-1)

Collection, identification, and enumeration of marine life remain a basic but daunting challenge in oceanography. Census of marine planktonic organisms, often by counting under a microscope, is a skilled yet slow, tedious, and unglamorous occupation, overdue for technological replacement. Larger mobile organisms create further challenges. The discovery that marine life leave behind "environmental DNA" or "eDNA" sequences that can be obtained from filtered seawater (to survey sea life from microbes to whales), coupled with the ability to collect and archive filtered water samples (i.e., Environmental Sample Processor or ESP), provides one approach (see Figure B3-2 for an example) that opens a new window into observing life in the sea. This is a fast developing field with many challenges ahead, but eDNA, together with other evolving optical and acoustical methods, may someday be used to semi-autonomously identify the multitude of organisms inhabiting a body of water.

FIGURE B3-1. Marine life from the Monterey Bay area and the means for autonomous observing. Organisms slough DNA into the water column, and exploratory studies are being conducted at MBARI to determine if such "eDNA" can be used to census a wide variety of Monterey Bay organisms. Figure B3-2 highlights an early success story. *Illustration by Kelly Lance, ©MBARI*

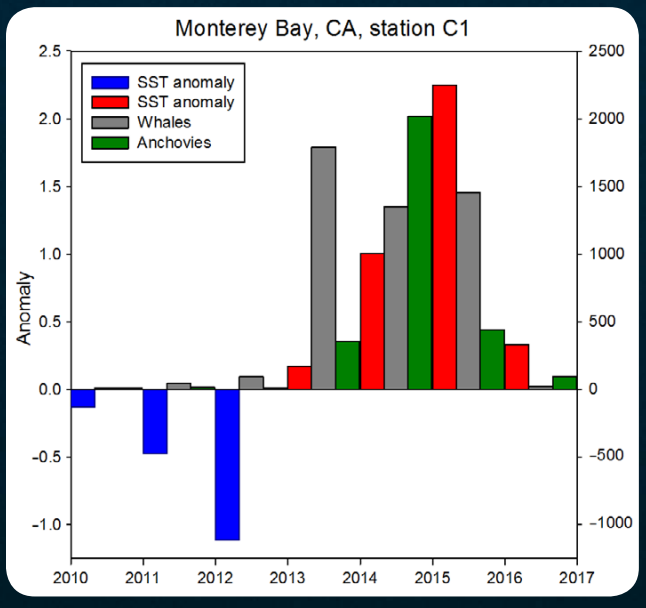

FIGURE B3-2. Filtered water samples from time-series station C1 archived in liquid nitrogen provided a unique opportunity to test the utility of eDNA. An unusual increase in the abundance of humpback whales occurred during the warm Blob and El Niño of 2013–2015. Remotely operated vehicle observations indicated the whales were feeding on anchovies. eDNA samples extracted from the time-series water samples were amplified with anchovy-specific polymerase chain reaction (PCR) primers (Sassoubre et al., 2016). Whale sightings, anchovy eDNA, and temperature anomalies show almost perfect accord—both animals were rare during the preceding cool years, and both were common during the warm years.

campaigns. Two important capabilities for the LRAUVs are under development: (1) water sampling capabilities (see Box 2), and (2) the adaptation of a new generation Environmental Sample Processor (ESP; see companion paper by Scholin et al., 2017, in this issue). As part of a Marine Biodiversity Observation Network project, we are opening a new window into observing life in the sea by developing ESP sampling for surveying marine biota from microbes to whales utilizing environmental DNA (see Box 3). In order to preserve the underway time series of pCO_2 (Figure 8), we recently completed incorporation of pCO_2 and pH sensors into an autonomous surface vehicle (the Liquid Robotics Wave Glider; Chavez et al., 2017). Our goal is to transition to a mostly autonomous time series in the near future (Figure 10).

Time series have routinely been established at specific geographical locations (i.e., HOT and BATS). In the open ocean, a single site was seen as representative of a broad spatial domain. Satellite remote sensing together with in situ data have now shown that these regions are anything but uniform. In coastal environments, spatial variability is further enhanced. In Monterey Bay, upwelling shapes almost every aspect of the ecosystem, from the regions of most active upwelling, to the strong fronts that form between the cool upwelled and the warmer surrounding waters, to the productive upwelling shadows and the offshore coastal transition zone waters. The fronts are areas of enhanced biological activity and trophic transfer, and our fixed-location time series often miss key aspects of these dynamics, confounding our interpretation of change. Should the process, rather than geography, determine the sampling location? With the advent of smart mobile autonomous systems that are fully integrated with remote sensing and other in situ observation systems such as moorings and real-time numerical models, we can begin to imagine a future of process-driven time series.

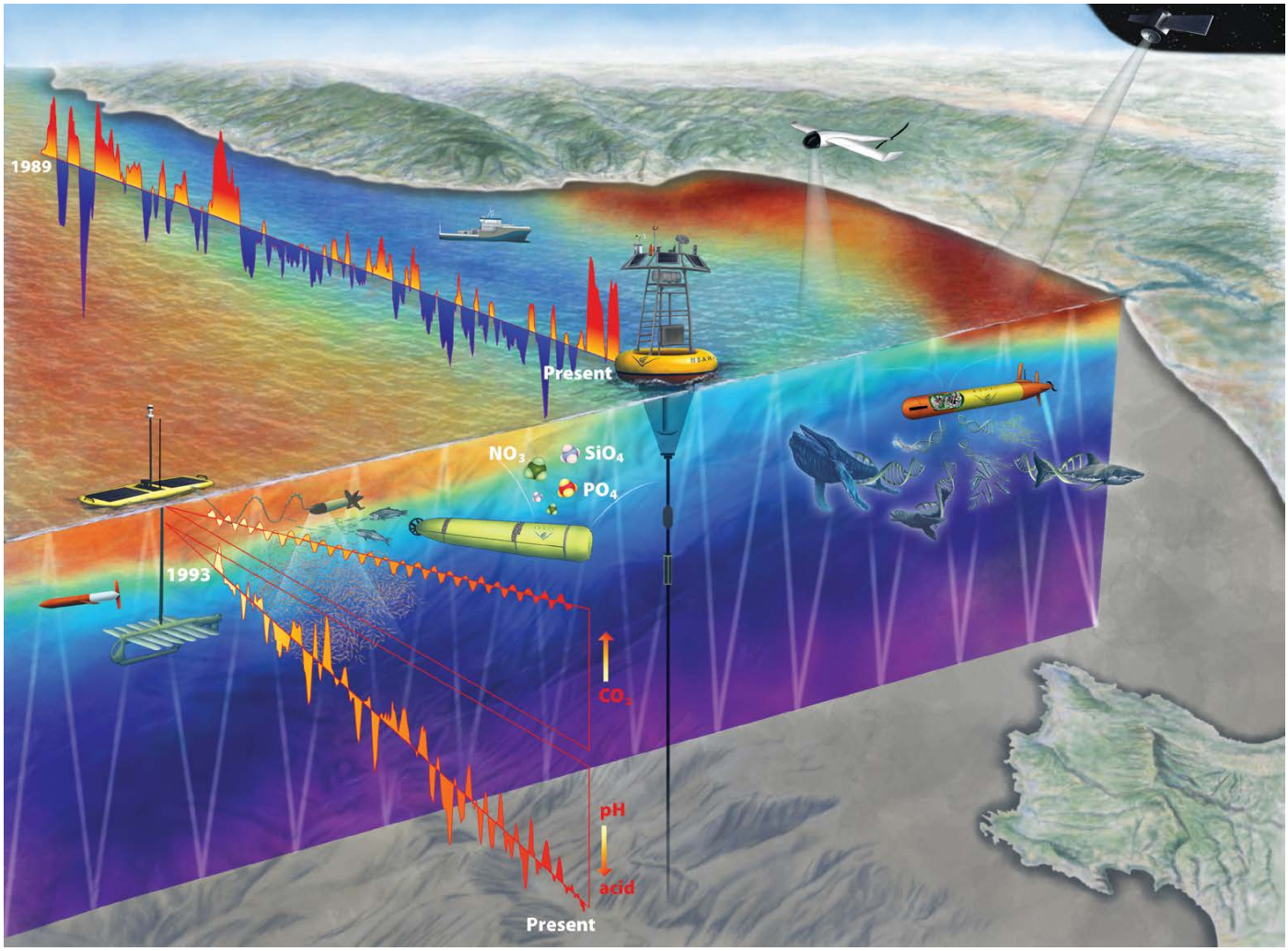

FIGURE 10. A full autonomy vision for the Monterey Bay time series. The underway pCO_2 time series is extended with measurements from an autonomous surface vehicle, the Liquid Robotics Wave Glider. Spray gliders measure temperature, salinity, oxygen, and fluorescence out to 300 km. The M1 mooring provides continuous measurements of physics, biogeochemistry, and biology. Autonomous vehicles provide high-resolution sections as well as return samples to shore for laboratory analysis. Satellites, and future drones, monitor the sea surface. Ships will continue to find use for process studies and new system developments. *Illustration by Kelly Lance, ©MBARI*

REFERENCES

Ashok, K., S.K. Behera, S.A. Rao, H. Weng, and T. Yamagata. 2007. El Niño Modoki and its possible teleconnection. *Journal of Geophysical Research* 112, C11007, https://doi.org/10.1029/2006JC003798.

Bakun, A. 1990. Global climate change and intensification of coastal ocean upwelling. *Science* 247:198–202, https://doi.org/10.1126/science.247.4939.198.

Barber, R.T., and F.P. Chavez. 1983. Biological consequences of El Niño. *Science* 222(4629):1,203–1,210, https://doi.org/10.1126/science.222.4629.1203.

Barber, R.T., and R.L. Smith. 1981. Coastal upwelling ecosystems. Pp. 31–68 in *Analysis of Marine Ecosystems*. A.R. Longhurst, ed., Academic Press, New York.

Barton, A., B. Hales, G. Waldbusser, C. Langdon, and R. Feely. 2012. The Pacific oyster, *Crassostrea gigas*, shows negative correlation to naturally elevated carbon dioxide levels: Implications for near-term ocean acidification effects. *Limnology and Oceanography* 57(3):698–710, https://doi.org/10.4319/lo.2012.57.3.0698.

Bellingham, J.G., Y. Zhang, J.E. Kerwin, J. Erikson, B. Hobson, B. Kieft, M. Godin, R. McEwen, T. Hoover, J. Paul, and others. 2010. Efficient propulsion for the *Tethys* long-range autonomous underwater vehicle. Paper presented at the 2010 IEEE/OES Autonomous Underwater Vehicles (AUV) conference, September 1–3, 2010, Monterey, California, https://doi.org/10.1109/AUV.2010.5779645.

Bjerknes, J. 1966. Survey of El Niño 1957-58 in its relation to tropical Pacific meteorology. *Inter-American Tropical Tuna Commission Bulletin* 12(2):1–62.

Bograd, S.J., C.G. Castro, E. Di Lorenzo, D.M. Palacios, H. Bailey, W. Gilly, and F.P. Chavez. 2008. Oxygen declines and the shoaling of the hypoxic boundary in the California Current. *Geophysical Research Letters* 35, L12607, https://doi.org/10.1029/2008GL034185.

Bond, N.A., M.F. Cronin, H. Freeland, and N. Mantua. 2015. Causes and impacts of the 2014 warm anomaly in the Northeast Pacific. *Geophysical Research Letters* 42:3,414–3,420, https://doi.org/10.1002/2015GL063306.

Brewer, P.G., K.W. Bruland, R.W. Eppley, and J.J. McCarthy. 1986. The Global Ocean Flux Study (GOFS): Status of the U.S. GOFS Program. *Eos, Transactions American Geophysical Union* 67(44):827–832, https://doi.org/10.1029/EO067i044p00827.

Brönnimann, S. 2005. The global climate anomaly, 1940–1942. *Weather* 60(12):336–342, https://doi.org/10.1256/wea.248.04.

Chavez, F.P. 1987. *Ocean Variability and Phytoplankton Community Structure*. PhD Dissertation, Duke University, Durham, North Carolina, 300 pp.

Chavez, F.P. 1989. Size distribution of phytoplankton in the central and eastern tropical Pacific. *Global Biogeochemical Cycles* 3:27–35, https://doi.org/10.1029/GB003i001p00027.

Chavez, F.P., R.T. Barber, A. Huyer, P.M. Kosro, S.R. Ramp, T. Stanton, and B. Rojas de Mendiola. 1991. Horizontal transport and the distribution of nutrients in the Coastal Transition Zone off northern California: Effects on primary production, phytoplankton biomass and species composition. *Journal of Geophysical Research* 96(C8):14,833–14,848, https://doi.org/10.1029/91JC01163.

Chavez, F.P., A. Bertrand, R. Guevara-Carrasco, P. Soler, and J. Csirke. 2008. The northern Humboldt Current System: Brief history, present status and a view towards the future. *Progress in Oceanography* 79(2–4):95–105, https://doi.org/10.1016/j.pocean.2008.10.012.

Chavez, F.P., and C.A. Collins. 1998. California Current System: Part 1. Preface. *Deep-Sea Research Part II* 45(8–9):1,407–1,409, https://doi.org/10.1016/S0967-0645(98)80001-5.

Chavez, F.P., and C.A. Collins. 2000. Studies of the California Current System: Present, past and future. *Deep Sea Research Part II* 47(5–6):761–763, https://doi.org/10.1016/S0967-0645(99)00125-3.

Chavez, F.P., C.A. Collins, A. Huyer, and D.L. Mackas. 2002a. El Niño along the west coast of North America. *Progress in Oceanography* 54(1):1–5, https://doi.org/10.1016/S0079-6611(02)00040-X.

Chavez, F.P., and M. Messié. 2009. A comparison of eastern boundary upwelling ecosystems. *Progress in Oceanography* 83(1):80–96, https://doi.org/10.1016/j.pocean.2009.07.032.

Chavez, F.P., M. Messié, and J.T. Pennington. 2011. Marine primary production in relation to climate variability and change. *Annual Review of Marine Science* 3:227–260, https://doi.org/10.1146/annurev.marine.010908.163917.

Chavez, F.P., J.T. Pennington, C.G. Castro, J.P. Ryan, R.P. Michisaki, B. Schlining, P. Walz, K.R. Buck, A. McFadyen, and C.A. Collins. 2002b. Biological and chemical consequences of the 1997–1998 El Niño in central California waters. *Progress in Oceanography* 54(1):205–232, https://doi.org/10.1016/S0079-6611(02)00050-2.

Chavez, F.P., J.T. Pennington, R. Herlien, H. Jannasch, G. Thurmond, and G.E. Friederich. 1997. Moorings and drifters for real-time interdisciplinary oceanography. *Journal of Atmospheric and Oceanic Technology* 14(5):1,199–1,211, https://doi.org/10.1175/1520-0426(1997)014<1199:MADFRT>2.0.CO;2.

Chavez, F.P., J. Ryan, S.E. Lluch-Cota, and M. Ñiquen. 2003. From anchovies to sardines and back: Multidecadal change in the Pacific Ocean. *Science* 299(5604):217–221, https://doi.org/10.1126/science.1075880.

Chavez, F.P., J. Sevadjian, C. Wahl, J. Friederich, and G.E. Friederich. 2017. Measurements of pCO_2 and pH from an autonomous surface vehicle in a coastal upwelling system. *Deep Sea Research Part II*, https://doi.org/10.1016/j.dsr2.2017.01.001

Chavez, F.P., P.G. Strutton, G.E. Friederich, R.A. Feely, G.C. Feldman, D.G. Foley, and M.J. McPhaden. 1999. Biological and chemical response of the equatorial Pacific Ocean to the 1997–98 El Niño. *Science* 286:2,126–2,131, https://doi.org/10.1126/science.286.5447.2126.

Chelton, D.B., and R.E. Davis. 1982. Monthly mean sea-level variability along the west coast of North America. *Journal of Physical Oceanography* 12(8):757–784, https://doi.org/10.1175/1520-0485(1982)012<0757:MMSLVA>2.0.CO;2.

Cleveland, W.S., A.E. Freeny, and T.E. Graedel. 1983. The seasonal component of atmospheric CO_2: Information from new approaches to the decomposition of seasonal time-series. *Journal of Geophysical Research* 88:10,934–10,940, https://doi.org/10.1029/JC088iC15p10934.

Collins, C.A, J.T. Pennington, C.G. Castro, T.A. Rago, and F.P. Chavez. 2003. The California Current System off Monterey, California: Physical and biological coupling. *Deep Sea Research Part II* 50(14–16):2,389–2,404, https://doi.org/10.1016/S0967-0645(03)00134-6.

Croll, D.A., B. Marinovic, S. Benson, F.P. Chavez, N. Black, R. Ternullo, and B.R. Tershy. 2005. From wind to whales: Trophic links in a coastal upwelling system. *Marine Ecology Progress Series* 289:117–130, https://doi.org/10.3354/meps289117.

Deutsch, C., W. Berelson, R. Thunell, T. Weber, C. Tems, J. McManus, J. Crusius, T. Ito, T. Baumgartner, V. Ferreira, and others. 2014. Centennial changes in North Pacific anoxia linked to tropical trade winds. *Science* 345(6197):665–668, https://doi.org/10.1126/science.1252332.

Di Lorenzo, E., N. Schneider, K.M. Cobb, K. Chhak, P.J.S. Franks, A.J. Miller, J.C. McWilliams, S.J. Bograd, H. Arango, E. Curchister, and others. 2008. North Pacific Gyre Oscillation links ocean climate and ecosystem change. *Geophysical Research Letters* 35, L08607, https://doi.org/10.1029/2007GL032838.

Elrod, V.A., K.S. Johnson, S.E. Fitzwater, and J.N. Plant. 2008. A long-term, high-resolution record of surface water iron concentrations in the upwelling-driven central California region. *Journal of Geophysical Research: Oceans* 113, C11021, https://doi.org/10.1029/2007JC004610.

Enfield, D.B., and J.S. Allen. 1980. On the structure and dynamics of monthly mean sea level anomalies along the Pacific Coast of North and South America. *Journal of Physical Oceanography* 10(4):557–578, https://doi.org/10.1175/1520-0485(1980)010<0557:OTSADO>2.0.CO;2.

England, M.H., S. McGregor, P. Spence, G.A. Meehl, A. Timmermann, W. Cai, A.S. Gupta, M.J. McPhaden, A. Purich, and A. Santoso. 2014. Recent intensification of wind-driven circulation in the Pacific and the ongoing warming hiatus. *Nature Climate Change* 4(3):222–227, https://doi.org/10.1038/nclimate2106.

Friederich, G.E., P.G. Brewer, R. Herlien, and F.P. Chavez. 1995. Measurement of sea surface partial pressure of CO_2 from a moored buoy. *Deep Sea Research Part I* 42:1,175–1,186, https://doi.org/10.1016/0967-0637(95)00044-7.

Graham, W.M., and J.L. Largier. 1997. Upwelling shadows as nearshore retention sites: The example of northern Monterey Bay. *Continental Shelf Research* 17:509–532, https://doi.org/10.1016/S0278-4343(96)00045-3.

Hickey, B.M. 1979. The California Current System: Hypothesis and facts. *Progress in Oceanography* 8:191–279, https://doi.org/10.1016/0079-6611(79)90002-8.

Hobson, B.W., J.G. Bellingham, B. Kieft, R. McEwen, M. Godin, and Y. Zhang. 2012. *Tethys*-class long range AUVs: Extending the endurance of propeller-driven cruising AUVs from days to weeks. Paper presented at the 2012 IEEE/OES Autonomous Underwater Vehicles (AUV) conference, September 24–27, 2012, Southampton, UK, https://doi.org/10.1109/AUV.2012.6380735.

Jaccard, S.L., E.D. Galbraith, T.L. Frölicher, and N. Gruber. 2014. Ocean (de)oxygenation across the last deglaciation: Insights for the future. *Oceanography* 27(1):26–35, https://doi.org/10.5670/oceanog.2014.05.

Jacox, M.G., E.L. Hazen, K.D. Zaba, D.L. Rudnick, C.A. Edwards, A.M. Moore, and S.J. Bograd. 2016. Impacts of the 2015–2016 El Niño on the California Current System: Early assessment and comparison to past events. *Geophysical Research Letters* 43(13):7,072–7,080, https://doi.org/10.1002/2016GL069716.

Jessup, D.A., M.A. Miller, J.P. Ryan, H.M. Nevins, H.A. Kerkering, A. Mekebri, D.B. Crane, T.A. Johnson, and R.M. Kudela. 2009. Mass stranding of marine birds caused by a surfactant-producing red tide. *PLoS ONE* 4(2):e4550, https://doi.org/10.1371/journal.pone.0004550.

Johnson, K.S., F.P. Chavez, V.A. Elrod, S.E. Fitzwater, J.T. Pennington, K.R. Buck, and P.M. Walz. 2001. The annual cycle of iron and the biological response in central California coastal waters. *Geophysical Research Letters* 28:1,247–1,250, https://doi.org/10.1029/2000GL012433.

Johnson, K.S., and L.J. Coletti. 2002. In situ ultraviolet spectrophotometry for high resolution and long-term monitoring of nitrate, bromide and bisulfide in the ocean. *Deep Sea Research Part I* 49:1,291–1,305, https://doi.org/10.1016/S0967-0637(02)00020-1.

Johnson, K.S., L.J. Coletti, and F.P. Chavez. 2006. Diel nitrate cycles observed with in situ sensors predict monthly and annual new production. *Deep Sea Research Part I* 53(3):561–573, https://doi.org/10.1016/j.dsr.2005.12.004.

Karl, D.M. 2010. Oceanic ecosystem time-series programs: Ten lessons learned. *Oceanography* 23(3):104–125, https://doi.org/10.5670/oceanog.2010.27.

Karl, D.M., and M.J. Church. 2014. Microbial oceanography and the Hawaii Ocean Time-series programme. *Nature Reviews Microbiology* 12:699–713, https://doi.org/10.1038/nrmicro3333.

Lluch-Belda, D., D.B. Lluch-Cota, and S.E. Lluch-Cota. 2003. Baja California's biological transition zones: Refuges for the California sardine. *Journal of Oceanography* 59(4):503–513, https://doi.org/10.1023/A:1025596717470.

MacIsaac, J.J., R.C. Dugdale, R.T. Barber, D. Blasco, and T.T. Packard. 1985. Primary production cycle in an upwelling center. *Deep Sea Research Part A* 32:503–529, https://doi.org/10.1016/0198-0149(85)90042-1.

Margalef, R. 1978. Life-forms of phytoplankton as survival alternatives in an unstable environment. *Oceanologica Acta* 1(4):493–509.

Martin, J.H., G.A. Knauer, D.M. Karl, and W.W. Broenkow. 1987. VERTEX: Carbon cycling in the Northeast Pacific. *Deep Sea Research Part A* 34(2):267–85, https://doi.org/10.1016/0198-0149(87)90086-0.

MBARI. 2010. A new coastal pelagic ecosystem paradigm? Pp. 9–11 in *Monterey Bay Aquarium Research Institute Annual Report 2010*. Moss Landing, CA.

McClatchie, S., R. Goericke, R. Cosgrove, G. Auad, and R. Vetter. 2010. Oxygen in the Southern California Bight: Multidecadal trends and implications for demersal fisheries. *Geophysical Research Letters* 37, L19602, https://doi.org/10.1029/2010GL044497.

Messié, M., and F.P. Chavez. 2011. Global modes of sea surface temperature variability in relation to regional climate indices. *Journal of Climate* 24(16):4,314–4,331, https://doi.org/10.1175/2011JCLI3941.1.

Olivieri, R.A., and F.P. Chavez. 2000. A model of plankton dynamics for the coastal upwelling system of Monterey Bay, California. *Deep Sea Research Part II* 47(5–6):1,077–1,106, https://doi.org/10.1016/S0967-0645(99)00137-X.

Paek, H., J.Y. Yu, and C. Qian. 2017. Why were the 2015/2016 and 1997/1998 extreme El Niños different? *Geophysical Research Letters* 44:1,848–1,856, https://doi.org/10.1002/2016GL071515.

Pares Sierra, A., and J.J. O'Brien. 1989. The seasonal and interannual variability of the California Current System: A numerical model. *Journal of Geophysical Research:* 94(C3):3,159–3,180, https://doi.org/10.1029/JC094iC03p03159.

Pennington, J.T., M. Blum, and F.P. Chavez. 2016. Seawater sampling by an autonomous underwater vehicle: "Gulper" sample validation for nitrate, chlorophyll, phytoplankton, and primary production. *Limnology and Oceanography: Methods* 14(1):14–23, https://doi.org/10.1002/lom3.10065.

Pennington, J.T., G.E. Friederich, C.G. Castro, C.A. Collins, W.W. Evans, and F.P. Chavez. 2010. The northern and central California coastal upwelling system. 2010. Pp. 29–43 in *Carbon and Nutrient Fluxes in Continental Margins: A Global Synthesis*. K.K. Liu, L. Atkinson, R. Quinones, and L. Talaue-McManus, eds, Springer Verlag Berlin Heidelberg.

Pennington, J.T, and F.P. Chavez. 2000. Seasonal fluctuations of temperature, salinity, nitrate, chlorophyll and primary production at Station H3/M1 over 1989-1996 in Monterey Bay, California. *Deep Sea Research Part II* 47(5–6):947–973, https://doi.org/10.1016/S0967-0645(99)00132-0.

Pennington, J.T, and F.P. Chavez. 2017. Decade-scale oceanographic fluctuation in Monterey Bay, California, 1989–2011. *Deep Sea Research Part II,* https://doi.org/10.1016/j.dsr2.2017.07.005.

Redfield, A.C. 1958. The biological control of chemical factors in the environment. *American Scientist* 46(3):230A, 205–221.

Ren, A.S. 2016. *Declining Dissolved Oxygen in the Central California Current Region*. MS Thesis, University of Maine, Orono, https://digitalcommons.library.umaine.edu/etd/2539.

Rosenfeld, L.K., F.B. Schwing, N. Garfield, and D.E. Tracy. 1994. Bifurcated flow from an upwelling center: A cold water source for Monterey Bay. *Continental Shelf Research* 14(9):931–964, https://doi.org/10.1016/0278-4343(94)90058-2.

Rudnick, D.L., K.D. Zaba, R.E. Todd, and R.E. Davis. 2017. A climatology of the California Current System from a network of underwater gliders. *Progress in Oceanography* 154:64–106, https://doi.org/10.1016/j.pocean.2017.03.002.

Ryan, J.P., F.P. Chavez, and J.G. Bellingham. 2005. Physical-biological coupling in Monterey Bay, California: Topographic influences on phytoplankton ecology. *Marine Ecology Progress Series* 287:23–32, https://doi.org/10.3354/meps287023.

Ryan, J.P., A.M. Fischer, R.M. Kudela, J.F.R. Gower, S.A. King, R. Marin III, and F.P. Chavez. 2009. Influences of upwelling and downwelling winds on red tide bloom dynamics in Monterey Bay, California. *Continental Shelf Research* 29(5–6):785–795, https://doi.org/10.1016/j.csr.2008.11.006

Ryan, J.P., J.F.R. Gower, S.A. King, W.P. Bissett, A.M. Fischer, R.M. Kudela, Z. Kolber, F. Mazzillo, E.V. Rienecker, and F.P. Chavez. 2008a. A coastal ocean extreme bloom incubator. *Geophysical Research Letters* 35, L12602, https://doi.org/10.1029/2008GL034081.

Ryan, J., D. Greenfield, R. Marin III, C. Preston, B. Roman, S. Jensen, D. Pargett, J. Birch, C. Mikulski, G. Doucette, and C. Scholin. 2011. Harmful phytoplankton ecology studies using an autonomous molecular analytical and ocean observing network. *Limnology and Oceanography* 56, https://doi.org/10.4319/lo.2011.56.4.1255.

Ryan, J.P., R.M. Kudela, J.M. Birch, M. Blum, H.A. Bowers, F.P. Chavez, G.J. Doucette, K. Hayashi, R. Marin III, C.M. Mikulski, and others. 2017. Causality of an extreme harmful algal bloom in Monterey Bay, California, during the 2014–2016 Northeast Pacific warm anomaly. *Geophysical Research Letters* 44:5,571–5,579, https://doi.org/10.1002/2017GL072637.

Ryan, J.P., M.A. McManus, R.M. Kudela, M. Lara Artigas, J.G. Bellingham, F.P. Chavez, G. Doucette, D. Foley, M. Godin, J.B.J. Harvey, and others. 2014. Boundary influences on HAB phytoplankton ecology in a stratification-enhanced upwelling shadow. *Deep Sea Research Part II* 101:63–79, https://doi.org/10.1016/j.dsr2.2013.01.017.

Ryan, J.P., M.A. McManus, J.D. Paduan, and F.P. Chavez. 2008b. Phytoplankton thin layers caused by shear infrontal zones of a coastal upwelling system. *Marine Ecology Progress Series* 354:21–34, https://doi.org/10.3354/meps07222.

Ryan, J.P., M.A. McManus, and J.M. Sullivan. 2010. Interacting physical, chemical and biological forcing of phytoplankton thin-layer variability in Monterey Bay, California. *Continental Shelf Research* 30:7–16, https://doi.org/10.1016/j.csr.2009.10.017.

Rykaczewski, R.R., and J.P. Dunne. 2010. Enhanced nutrient supply to the California Current ecosystem with global warming and increased stratification in an earth system model. *Geophysical Research Letters* 37, L21606, https://doi.org/10.1029/2010GL045019.

Ryther, J.H. 1969. Photosynthesis and fish production in the sea. *Science* 166(3901):72–76, https://doi.org/10.1126/science.166.3901.72.

Sakamoto, C.M., K.S. Johnson, L.J. Coletti, T.L. Maurer, G. Massion, J.T. Pennington, J.N. Plant, H.W. Jannasch, and F.P. Chavez. 2017. Hourly in situ nitrate on a coastal mooring: A 15-year record and insights into new production. *Oceanography* 30(4):114–127, https://doi.org/10.5670/oceanog.2017.428.

Sassoubre, L.M., K.M. Yamahara, L.D. Gardner, B.A. Block, and A.B. Boehm. 2016. Quantification of environmental DNA (eDNA) shedding and decay rates for three marine fish. *Environmental Science & Technology* 50:10,456–10,464, https://doi.org/10.1021/acs.est.6b03114.

Scholin, C.A., J. Birch, S. Jensen, R. Marin III, E. Massion, D. Pargett, C. Preston, B. Roman, and W. Ussler III. 2017. The quest to develop ecogenomic sensors: A 25-Year history of the Environmental Sample Processor (ESP) as a case study. *Oceanography* 30(4):100–113, https://doi.org/10.5670/oceanog.2017.427.

Scofield, W.L. 1926. The sardine at Monterey: Dominant size-class and their progression, 1919–1923. *California Fish and Game Commission, Fish Bulletin* 2:191–221.

Scofield, W.L. 1929. Sardine fishing methods at Monterey, California. *California Fish and Game Commission, Fish Bulletin* 19:61.

Sette, O.E., and J.D. Isaacs, eds. 1960. Proceedings of Symposium on "The Changing Pacific Ocean in 1957 and 1958," Rancho Santa Fe, CA, June 2–4, 1958. *California Cooperative Oceanic Fisheries Investigations Reports*, vol. VII, January 1958 to June 1959, 217 pp.

Skogsberg, T. 1936. Hydrography of Monterey Bay, California: Thermal conditions, 1929–1933. *Transactions of the American Philosophical Society* 29(1):i–152, https://doi.org/10.2307/1005510.

Strub, P.T., and C. James. 2000. Altimeter-derived variability of surface velocities in the California Current system: Part 2. Seasonal circulation and eddy statistics. *Deep Sea Research Part II* 47(5):831–870, https://doi.org/10.1016/S0967-0645(99)00129-0.

Sutton, A.J., R.A. Feely, C.L. Sabine, M.J. McPhaden, T. Takahashi, F.P. Chavez, G.E. Friederich, and J.T. Mathis. 2014. Natural variability and anthropogenic change in equatorial Pacific surface ocean pCO_2 and pH. *Global Biogeochemical Cycles* 28:131–145, https://doi.org/10.1002/2013GB004679.

Zeidberg, L.D., and B.H. Robison. 2007. Invasive range expansion by the Humboldt squid, *Dosidicus gigas*, in the eastern North Pacific. *Proceedings of the National Academy of Sciences of the United States of America* 104:12,948–12,950, https://doi.org/10.1073/pnas.0702043104.

ACKNOWLEDGMENTS

Our group's sustained and broad-based data collections over the past 30 years have produced a deep and continually updated data library from which fundamental insights emerge. We are extremely grateful to the David and Lucile Packard Foundation, as these programs could never have been sustained with short-run government grants. Support from the National Aeronautics and Space Administration, the National Oceanic and Atmospheric Administration, and the National Science Foundation have supplemented sample collection and analysis as well as development of new methods.

AUTHORS

Francisco P. Chavez (chfr@mbari.org) is Senior Scientist, **J. Timothy Pennington** is Senior Research Specialist, **Reiko P. Michisaki** is Senior Research Technician, **Marguerite Blum** is Research Technician, **Gabriela M. Chavez** was a summer intern, **Jules Friederich** is Research Assistant, **Brent Jones** is Engineer, **Robert Herlien** is Software Engineer, **Brian Kieft** is Software Engineer, **Brett Hobson** is Mechanical Engineer, **Alice S. Ren** was a summer intern, **John Ryan** is Senior Research Specialist, **Jeffrey C. Sevadjian** was Research Technician, **Christopher Wahl** is Operations Engineer, **Kristine R. Walz** is Research Assistant, **Kevan Yamahara** is Research Specialist, **Gernot E. Friederich** was Senior Research Specialist, and **Monique Messié** is Research Specialist, all at the Monterey Bay Aquarium Research Institute, Moss Landing, CA, USA.

ARTICLE CITATION

Chavez, F.P., J.T. Pennington, R.P. Michisaki, M. Blum, G.M. Chavez, J. Friederich, B. Jones, R. Herlien, B. Kieft, B. Hobson, A.S. Ren, J. Ryan, J.C. Sevadjian, C. Wahl, K.R. Walz, K. Yamahara, G.E. Friederich, and M. Messié. 2017. Climate variability and change: Response of a coastal ocean ecosystem. *Oceanography* 30(4):128–145, https://doi.org/10.5670/oceanog.2017.429.